



## Analytical study of photovoltaic thermal compound parabolic concentrator active double slope solar distiller with a helical coiled heat exchanger using CuO nanoparticles

Dharamveer\*, Samsheer, Anil Kumar

*Department of Mechanical Engineering, Delhi Technological University, Delhi, India-110042, Tel. +91 9760521551; email: veerdharam76@gmail.com (Dharamveer), Tel. +91 9818883689; email: samsheer@dce.ac.in (Samsheer), Tel. +91 9425680448; email: anilkumar76@dtu.ac.in (Anil Kumar)*

Received 18 February 2021; Accepted 16 June 2021

---

### ABSTRACT

An analytical study for double slope solar still with 25% covered photovoltaic thermal compound concentrator collector with helically coiled heat exchanger has been carried out for the proposed system (N-PVT-CPC-DS-HE). The nanoparticles are emergent fluids and thermal energy carriers due to their thermophysical and optical properties. The performance is carried out using water-loaded nanoparticles for the concentration of 0.25% for four collectors ( $N = 4$ ) in 280 kg mass basin fluid and flow rate being 0.02 kg/s. In the present study, the proposed system and previous system are taken. The performance of the proposed system is observed to be an additional higher compared to the previous system. The average thermal energy gain of 13.68%, average thermal exergy gain of 7.31%, and average yield gain of 16.31% appeared higher in the proposed system than the previous system. The utilization of CPC further increases the water temperature in the east and west sides up to a maximum of 4.37°C and a minimum of 1.64°C. The 25% covered PVT produces 97.6% excess electricity that can be utilized for other supportive applications. The optimum level of mass flow rate achieved is 0.02 kg/s which is 33% less than the previous 0.03 kg/s.

*Keywords:* Active solar distiller unit; CuO nanoparticles; Heat exchanger; Exergy of thermal; N-PVT-CPC-DS-HE

---

### 1. Introduction

Everyone is aware of the water crisis in the world. As the population is increasing day by day, water demand is also increasing in parallel. Water is freely available in considerable amounts in different forms. However, as drinkable water availability is concerned, only 0.97% of water availability is potable. Therefore, the production of potable water must increase. Many researchers are working toward increasing potable water production, but still much more work needs to be done. The present research is to enhance the generation of drinking water with the help of a solar distiller unit. Delyannis [1] and Tiwari et al. [2]

studied the historical developments of solar desalination taking care of energy and the environment. Dev et al. [3–7] developed characteristic equations for active and passive solar distiller units. In an active solar distiller unit, solar energy is fed to water as external thermal energy, and water is pumped mechanically in forced mode by using solar energy with the help of photovoltaic technology to improve the passive solar distiller. Soliman [8] recommended the concept of feeding external thermal energy from the solar collector into the basin. Rai and Tiwari [9] analyzed the effect of mass flow rate with solo basin solar distillation system attached with flat plate collector and observed a decrease in yield. Lawrence and Tiwari [10] calculated active solar distiller

---

\* Corresponding author.

in natural type with heat exchanging to extend empirical formulas. They observed that the addition of a collector increases the water temperature, which improves the system's efficiency; overall while increasing water depth decreases efficiency. Kumar and Tiwari [11] have optimized active double slope solar distiller units and got the highest water generation on a 1.8 m/s flow rate. Gaur and Tiwari [12] analyzed the maximum yield for four ( $N = 4$ ) collectors and 50 kg mass of fluid of hybrid solar still. Shyam et al. [13] developed an expression for connected N-PVT-water collectors for temperature-dependent electrical efficiency of two different configurations in series that gives almost identical outcomes. Later on, experiments were performed Shyam [14] for validation which found excellent conformity in these two studies. Boukar and Harmim [15] expressed the equations for perpendicular solar distillation systems. Dev and Tiwari [16] developed a thermal model of EISS, its validation with experimental results, and to compare the performance of EISS with the single slope. Tiwari and Sahota [17] analyzed the detailed review of energy and economic efficiencies of solar stills for different solar distiller units' (passive and active) characteristic equations. The various features of the nanofluids are the ultrafast heat transfer fluid, low friction coefficient, better stability, low pumping power, superior lubrication, and erosion that can improve unit performance and be observed as a thermal energy carrier. Furthermore, by changing the size and shape of the nanoparticles, they can be made more attractive for a variety of applications. Khairul et al. [18] investigated theoretically CuO, Al<sub>2</sub>O<sub>3</sub>, ZnO water-loaded nanofluids and concluded that heat transfer coefficient increases and entropy decreases. Mahian et al. [19] examined solar collector performance on the basis of the micro-channel using CuO, Al<sub>2</sub>O<sub>3</sub>, TiO<sub>2</sub> and SiO<sub>2</sub> nanofluids and found that the output temperature follows the order: CuO > TiO<sub>2</sub> > Al<sub>2</sub>O<sub>3</sub> > SiO<sub>2</sub> and also observed that the generation of entropy decreases. Mwesigye et al. [20] analyzed computationally that the nanofluid has a greater yield for passive double slope solar distiller units. Tripathi and Tiwari [21] studied the comparison between N-PVT-FPC and PVT-CPC. Atheaya et al. [22] developed a characteristic mathematical expression for a partly roofed PVT compound parabolic concentrator (CPC). Dharamveer et al. [23] presented a review on nanofluids with an active solar distiller unit which concluded that nanofluids reduce pump work by reducing viscosity and increases water generation. Dubey and Tiwari [24] Analyzed serially connected PVT flat plate water collectors. Popiel and Wojtkowiak [25] developed the formulas for the thermophysical properties of water. Raja Sekhar and Sharma [26] studied specific heat, viscosity for Al<sub>2</sub>O<sub>3</sub> nanofluids. Yiamsawasd et al. [27] studied specific heat of nanofluids. Pak and Cho [28] studied hydrodynamic and heat transfer of dispersed fluids with submicron metallic oxide particles. Khanafer and Vafai [29] studied a critical synthesis of thermophysical characteristics of nanofluids. Patel et al. [30] investigated experimentally thermal conductivity enhancement in oxide and metallic nanofluids. Sharma et al. [31] developed mathematical relations to find the friction and forced convection heat transfer coefficients of water-based nanofluids for turbulent flow in a tube. Wang et al. [32] studied turbulent flow in pipes for

particular reference of the transition area between smooth and rough pipe flows. Ho et al. [33] simulated natural convection of nanofluid in a square enclosure: uncertainties of viscosity and thermal conductivity. Mahian et al. [34] studied the entropy generation during Al<sub>2</sub>O<sub>3</sub> water nanofluid flow in a solar collector and different thermophysical models. Colebrook [35] studied turbulent flow in pipes, for particular reference of the transition area between smooth and rough pipe flows. Tiwari and Tiwari [37] studied solar distillation practice for water desalination systems. Tiwari [38] developed solar energy: fundamentals, design, modeling, and applications. Dharamveer and Samsheer [39] analyzed energy matrices and enviro-economics for active and passive solar distiller units comparatively. Balan, et al. [40] Review on passive solar distillation. Prasad et al. [41] N-PVT-CPC system analyzed using one at a time technique (OAT). Sharma et al. [42] analyzed a theoretical double slope solar distiller unit with parabolic concentrator ETC based on efficiency and matrices. Bharti et al. [43] examined the sensitivity analysis of  $N$  alike PVT flat plate collectors double slope solar distiller. Singh et al. [44] investigated; various efficiencies and productivity of  $N$  identical partially covered PVT flat plate collectors with single slope solar distiller units at different water depths under optimized conditions. Singh et al. [45] presented various unique designs on behalf of economic self-sustainability. Singh et al. [46] analyzed energy payback time for  $N$  identical compound parabolic concentrator collector with a single slope. Sharma et al. [47] observed the value of the exergoeconomic parameter decrease with an increased mass flow rate value. Gupta et al. [48] discussed fully covered  $N = 6$  CPC collectors and developed characteristic equations. Singh et al. [49] reviewed solar distillation systems with nanofluids. Sahota and Tiwari [50] analyzed exergoeconomic and enviroeconomic with or without heat exchanger double slope solar distiller unit loaded with nanofluid. Sahota et al. [51] studied and gives the maximum amount of the internal coefficient of evaporative heat transfer (HTC), which gives a high rate of water generation compared to the other distiller units. The characteristic curve for (N-PVT-FPC-DS-HE) is based on nanofluid. Nevertheless, no literature is obtainable on active solar distiller units (N-PVT-CPC-DS-HE) based on nanofluid. The current study presents an active photovoltaic thermal compound parabolic concentrator collector double slope solar distiller with a helically coiled heat exchanger using the CuO-nanoparticles.

## 2. System description

A schematic diagram of the proposed system is shown in Fig. 1, 1a–c and the previous system in Fig. 2. The proposed system is comprised of  $N$ th identically 25% enclosed photovoltaic thermal compound parabolic concentrator collector active double slope solar distiller using a helically coiled heat exchanger (N-PVT-CPC-DS-HE). The heat exchanger has dipped adequately in the basin, which is oriented in east and west. The basin is made of toughened glass with an inclination of top cover being 30°, and the basin area of fiber-reinforced plastic is  $2 \times 1$  m<sup>2</sup>. N-PVT-CPCs have a south-facing inclination of 45°. PVT generates electricity which operates on the D.C. motor

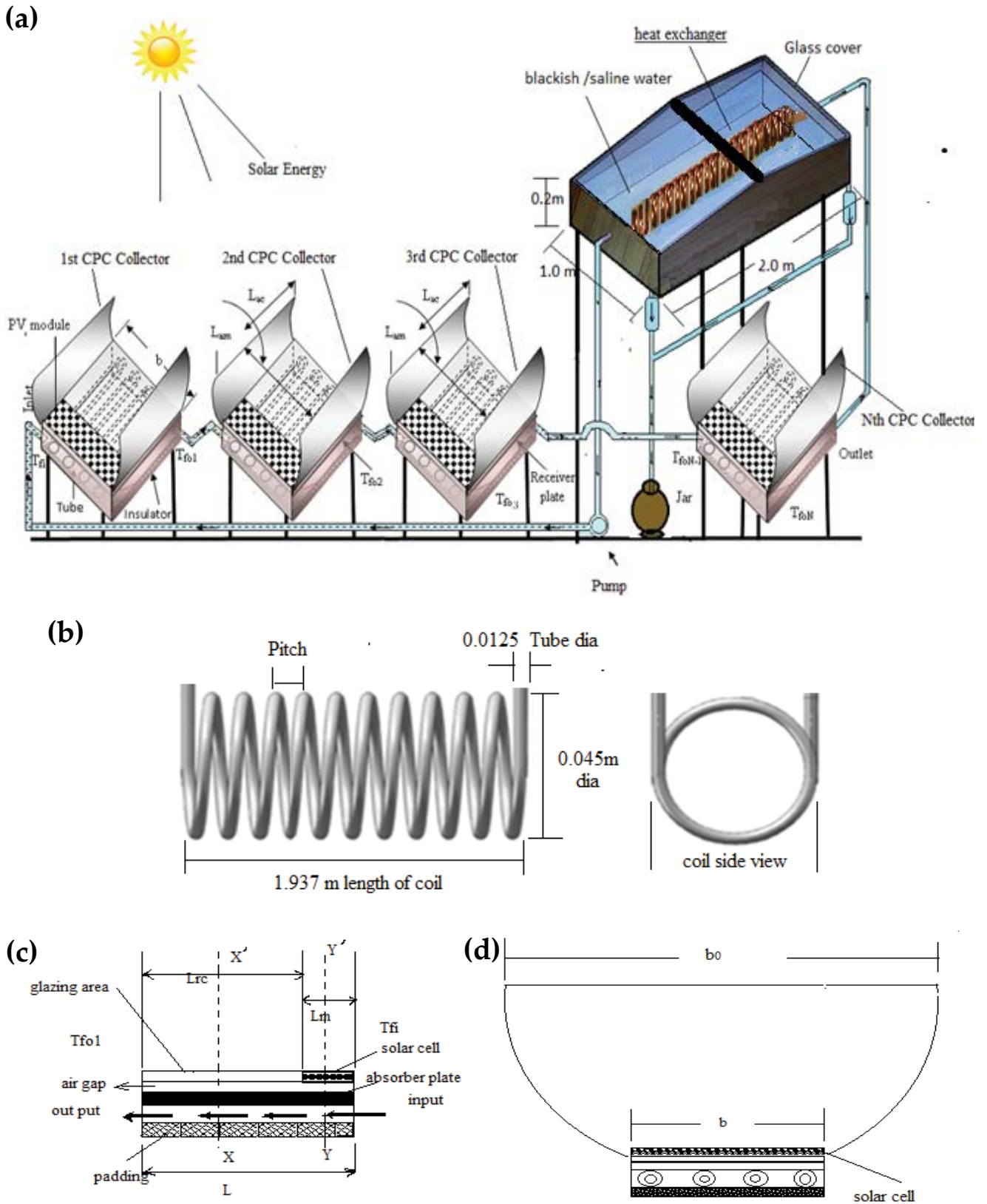


Fig. 1. Active  $N$ -identical 25% enclosed PVT-CPC-HE double slope distiller unit. (a) View of the helically coiled heat exchanger, (b) sectioned view of 25% enclosed  $N$ -PVT-CPC, and (c) cut section  $YY$  elevation of 25% covered  $N$ -PVT-CPC.

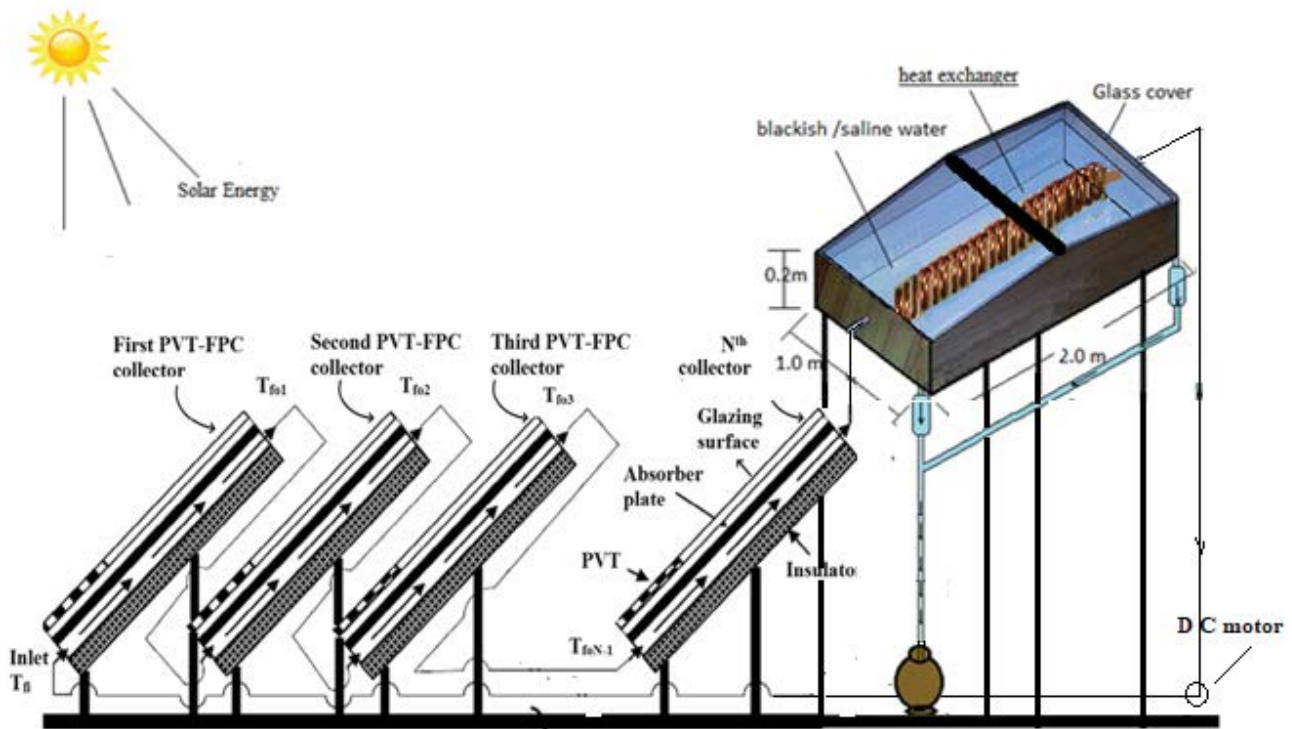


Fig. 2. Active double slope distiller  $N$ -identical 25% enclosed PVT-FPC-HE collectors.

as well as the pump. It has a fixed and accurate place for heat exchanging devices as per the basin water depth. The double slope distiller base sides are dyed mat black. The complete specification of the system is specified in Table 1. In this study, a system is proposed with a partly covered CPC collector constructed as in Fig. 1 and  $A_a > A_r$ ,  $L_{rm} = 0.25$  m and  $L_{rc} = 0.75$  m. A glazed flat plate collector is partly covered, and the remaining area is considered as the receiver area ( $A_r$ ). The aperture gets radiation from the beam reflected on the PVT collector, and the semi-transparent PV module is below the flat plate collector (FPC). The collector is shown in Fig. 1b and c. This transformation of thermal energy raises water temperature.

The intensity of solar via fluid of basin (BF/NF) directly penetrates the distiller unit's blackened surface, which is absorbed on basin liner. The irradiation gets thermally stored and raises the basin water temperature. The nanoparticles' electromagnetic wave produces intense absorption that interacts and produces mutual oscillation as Plasmon response. In the infrared and ultraviolet region, the Plasmon response of NPs has high modes. The higher concentration of nanoparticles is increased to a large basin surface area and increases the temperature of the heat exchanger. When latent heat is released, vapor gets condensed and collected into the jar. Due to this, the system becomes complex but enhances production. Due to the sedimentation and dispersion of nanoparticles, the system demands more maintenance. Advanced and classy tools are needed to eliminate the problems. Various separation methods have been developed, which depend on dimension, geometry, and a fraction of volume. Therefore, sets of NPs are required to reuse after rejecting brine for

an extended period as per the requirement to avoid the complexity of the additional saline water. The previous system is also an active double slope solar distiller unit of photovoltaic thermal  $N$ th identically 25% covered flat plate collector with helically coiled heat exchanger (N-PVT-FPC-DS-HE) (Fig. 2). The specifications of both the systems are the same except the compound parabolic collector, which is attached to the proposed system. The basin size ( $2 \times 1$ ) and mass of water is taken into consideration at 280 kg while 100 kg by the previous researcher [51]. The orientation of the double slope basin is from the east-west side, and the flat plate collectors are facing south. So, the maximum amount of solar energy can be absorbed by the distiller unit. In the proposed system,  $N$ th compound parabolic collectors are coupled with basin, while in the previous system,  $N$ th flat plate collectors are coupled with basin.

### 3. Mathematical formulation

The mathematical formulation is to express the balancing equations for various unit elements while taking all types of heat transfer. Following assumptions are taken by Sahota and Tiwari [50] and developed the characteristic equation to the unit as given below.

- The solar still is in quasi-steady-state (N-PVT-CPC-DS-HE).
- Neglect the ohmic losses from solar cells.
- The solar distiller unit is vapor leakproof.
- The water level is stable.
- The condensation is film-wise over the entire surface of the glass.

Table 1  
Different parameters used in calculations [22,51]

Parameters	Numerical values	Parameters	Numerical values
$\alpha_g$	0.050	$A_m$	0.6050
$\alpha_b$	0.80	$A_c$	1.3950
$\alpha_{bf}$	0.90	$L_p$	0.0020
$\alpha_c$	0.90	$K_m$	64.0 W/m K
$\alpha_p$	0.80	$K_p$	64.0 W/m K
$\beta$	0.890	$L_i$	0.10 m
$K_g$	0.780 W/m K	$h_i$	5.7 W/m <sup>2</sup> K
$K_b$	0.035 W/m K	$h_0$	9.5 W/m <sup>2</sup> K
$K_p$	0.166 W/m K	$U_{tcp}$	5.58 W/m <sup>2</sup> K
$L_g$	0.004	$U_{tca}$	9.20 W/m <sup>2</sup> K
$L_c$	0.005	$U_{tpa}$	4.74 W/m <sup>2</sup> K
$L_i$	0.1	$U_{lm}$	7.58 W/m <sup>2</sup> K
$\beta_0$	0.0045 K	$U_{lc}$	4.52 W/m <sup>2</sup> K
$x$	0.33 m	$PF_1$	0.378
$\sigma$	$5.670 \times 10^{-8}$ (W/m <sup>2</sup> K <sup>4</sup> )	$PF_2$	0.934
$\tau_g$	0.95	$PF_c$	0.955
$F'$	0.968	$\epsilon_g$	0.95
$\eta_0$	0.15	$\epsilon_{bf}$	0.95
Nanoparticle's thermal properties used (metallic CuO)			
Metallic NPs	Nanoparticle's density (kg/m <sup>3</sup> )	Specific heat $C_p$	Heat conductivity $k_p$ (W/m K)
CuO	$6.31 \times 10^3$	550	17.6
Technical specifications of active solar distiller unit (N-PVT-CPC-DSSS) [22]			
Active solar distiller unit (double slope)			
Components	Specifications		
Length	2.0 m		
Width	1.0 m		
Glass inclined	15°		
Low side high	0.20 m		
Body's material	GRP		
Stand's material	G.I.		
Cover's matter	Glass		
Orientation	East to west		
Thickness of glass cover	0.004 m		
Conductivity of glass $K_g$	0.816 W/m K		
Insulation thickness	0.10 m		
Insulation thermal conductivity	0.166 W/m K		
PVT-CPC collector [22]			
Components	Specifications	Components	Specifications
Collectors and types	$N = 4$ , tube and plate type	Area of aperture	2.0 m <sup>2</sup>
Receiving area of collector	1.0 m × 1.0 m	Module area	0.50 m × 2.0 m
Collector plate thickness	0.002 m	Receiver area	0.750 m × 2.0 m
Thickness of Cu tube	0.00056 m	Module receiving area	0.250 m × 1.0 m
Each Cu tubes length	1.0 m	Collector receiving area	0.750 m × 1.0 m
$K_i$	0.1660 (W/m K)	$F'$	0.9680
FF	0.80	$\rho$	0.840
Insulation thickness	0.10 m	$\tau_g$	0.950
CPC angle with horizontal	30°	$\alpha_c$	0.90
Thickness of glass on CPC	0.0040 m	$\beta_c$	0.890
Under glass collector effective area	0.75 m <sup>2</sup>	$\alpha_p$	0.80
Pipe dia.	0.0125 m	Under PV module effective area of collector	0.25 m <sup>2</sup>
DC motor	12 V, 24 W		

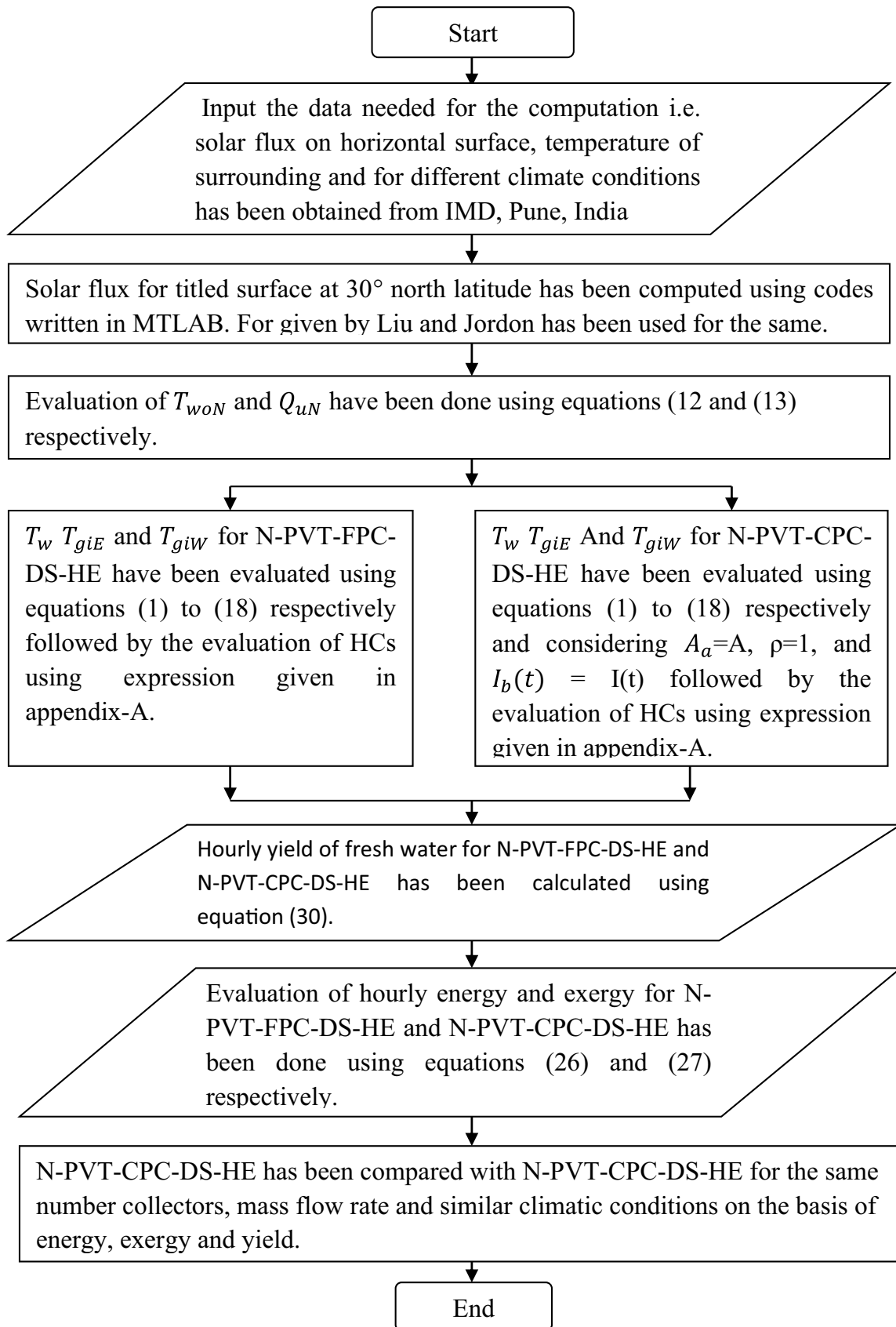


Fig. 3. The flow chart shows the methodology used.

3.1. Governing equations of energy for various part of the distiller unit of active double slope Nth identical (PVT-CPC-DS-HE) with the heat exchanger of the helically coiled system

3.1.1. Energy balance equation double slope solar basin [51]

- East face

$$\alpha_g \times I_{SE} \times A_{gE} + h_{1wE} \times (T_w - T_{giE}) \times \frac{A_b}{2} - h_{EW} \times (T_{giE} - T_{giW}) \times A_{gE} = U_{cgaE} \times (T_{giE} - T_a) \times A_{gE} \quad (1)$$

- West face

$$\alpha_g \times I_{SW} \times A_{gW} + h_{1wW} \times (T_w - T_{giW}) \times \frac{A_b}{2} + h_{EW} \times (T_{giE} - T_{giW}) \times A_{gW} = U_{cgaW} \times (T_{giW} - T_a) \times A_{gW} \quad (2)$$

On solving Eqs. (1) and (2):

$$T_{giE} = \frac{A_1 + A_2 \times T_w}{P} \quad (3)$$

$$T_{giW} = \frac{B_1 + B_2 \times T_w}{P} \quad (4)$$

$$T_{goE} = \frac{\frac{K_g}{L_g} T_{giE} + h_{1gE} T_a}{\frac{K_g}{L_g} + h_{1gE}} \quad (5)$$

$$T_{goW} = \frac{\frac{K_g}{L_g} T_{giW} + h_{1gW} T_a}{\frac{K_g}{L_g} + h_{1gW}} \quad (6)$$

The unknown terms,  $A_1$ ,  $A_2$ ,  $B_1$ ,  $B_2$ , and  $P$  in Eqs. (3)–(6) are mentioned in Appendix A:

- Basin liner

$$\alpha_b (I_{SE} + I_{SW}) + 2h_{bw} (T_b - T_w) + 2h_{ba} (T_b - T_a) \quad (7)$$

- Water equation

$$m_f C_f \frac{dT_w}{dt} = \alpha_w (I_{SE} + I_{SW}) \frac{A_b}{2} + 2h_{bw} (T_b - T_w) \frac{A_b}{2} - h_{1wE} (T_w - T_{giE}) \frac{A_b}{2} - h_{1wW} (T_w - T_{giW}) \frac{A_b}{2} + Q_{uN} \quad (8)$$

3.1.2. Equations of energy balance for heat exchanger are immersed in basin water (BF/NF) of solar distiller unit can be shown as

$$m_f C_f \frac{dT_w}{dx} d_x = -(2\pi r_{11} \times U) \times (T_{HE} - T_w) \times d_x \quad (9)$$

Applying the boundary conditions  $T_w$  at  $(x = 0) = T_{woN}$  and  $T_w$  at  $(x = L) = T_{wi}$  on solving we get:

$$T_{wi} = T_{HE} \left[ 1 - \exp\left(\frac{-2\pi r_{11} UL}{m_f C_f}\right) \right] + T_{woN} \exp\left(\frac{-2\pi r_{11} UL}{m_f C_f}\right) \quad (10)$$

$$\text{where } U = \left[ \frac{1}{h_{bf}} + \left( \frac{r_{11}}{k_1} \right) \ln\left( \frac{r_{22}}{k_1} \right) \left( \frac{1}{h_{bf}} \right) \right]^{-1}$$

3.1.3. Equation of energy balance for N-PVT-CPC water collectors is as

$$T_{woN} = \left[ \frac{(AF_R(\alpha\tau))_1 (1 - K_p^N)}{m_f C_f (1 - K_p)} \right] I_b + \left[ \frac{(AF_R(UL))_1 (1 - K_p^N)}{m_f C_f (1 - K_p)} \right] T_a + T_{wi} K_m^N \quad (11)$$

By solving the Eqs. (10) and (11) we get:

$$T_{woN} = \left[ \frac{(AF_R(\alpha\tau))_1 (1 - K_p^N) \left( \frac{1}{(1 - e^{-z} K_m^N)} \right)}{m_f C_f (1 - K_p)} \right] I_b + \left[ \frac{(AF_R(UL))_1 (1 - K_p^N) \left( \frac{1}{(1 - e^{-z} K_m^N)} \right)}{m_f C_f (1 - K_p)} \right] T_a + T_{HE} \quad (12)$$

Now from heat energy gain is computed using the following relation N-PVT-CPC-DS-HE.

$$Q_{uN} = m_f C_f (T_{woN} - T_{wi}) \quad (13)$$

From Eqs. (12) and (13) the water output temperature of N-PVT-CPC collector is  $T_{HE} > T_{wi} > T_w$ :

$$Q_{uN} = \left[ \frac{(AF_R \times (\alpha\tau))_1 (1 - K_p^N) \left( \frac{1}{(1 - e^{-z} K_m^N)} \right)}{(1 - K_p)} \right] I_b + \left[ \frac{(AF_R(UL))_1 (1 - K_p^N) \left( \frac{1}{(1 - e^{-z} K_m^N)} \right)}{(1 - K_p)} \right] T_a + m_f C_f [T_{HE} - T_{wi}] \quad (14)$$

$$Q_{uN} = [D_1 I_b + D_2 T_a + D_3] \quad (15)$$

where the unknown terms  $D_1$ ,  $D_2$  and  $D_3$  are given in appendix.

By putting  $T_{giE}$ ,  $T_{giW}$ ,  $2h_{bw} (T_b - T_w)$ , and  $Q_{uN}$  from Eqs. (3), (4) and (15) in Eq. (8):

$$\frac{dT_w}{dt} = -\frac{T_w}{m_f C_f} \left[ \frac{2h_{bw} \frac{A_b}{2} + h_{1wE} \left( 1 - \frac{A_1 + A_2}{P} \right) \frac{A_b}{2} + h_{1wW} \left( 1 - \frac{B_1 + B_2}{P} \right) \frac{A_b}{2} - D_3}{\left[ \frac{I_b}{m_f C_f} (2h_{bw} + D_1) \frac{A_b}{2} + \frac{\left\{ \alpha_w (I_{SE} + I_{SW}) \frac{A_b}{2} \right\} + D_2 T_a}{m_f C_f} \right]} \right] \quad (16)$$

$$\frac{dT_w}{dt} = -a_2 T_w + f_2(t)$$

Or

$$\frac{dT_w}{dt} + a_2 T_w = f_2(t)$$

where

$$a_2 = \frac{1}{m_f C_f} \left[ 2h_{bw} \frac{A_b}{2} + h_{1wE} \left( 1 - \frac{A_1 + A_2}{P} \right) \frac{A_b}{2} + \left[ h_{1wW} \left( 1 - \frac{B_1 + B_2}{P} \right) \frac{A_b}{2} - D_3 \right] \right]$$

$$f_2(t) = \frac{I_b}{m_f C_f} (2h_{bw} + D_2) \frac{A_b}{2} + \frac{\left\{ \alpha_w (I_{SE} + I_{SW}) \frac{A_b}{2} \right\} + D_2 T_a}{m_f C_f}$$

$$\frac{dT_w}{dt} = \frac{f_2(t)}{a_2} (1 - e^{-a_2 \Delta t}) + T_{w0} e^{-a_2 \Delta t}$$

where  $T_{w0}$  is basin water temperature at  $t = 0$ ;  $f_2(t)$  is mean value of  $f_2(t)$  at  $t = 0$  and  $t$ .

Further, by using Tables 2 and 3 for thermophysical properties and coefficient of heat transfer from Table 4, and the per hour temperature variation of basefluid and CuO-nanoparticles (BF/NF) [31] of the distiller unit can be obtained by Eq. (18) on substituting  $T_{giE}$ ,  $T_{giW}$  and  $T_w$  in the equation:

$$\eta_{gth} = \frac{h_{1wE} (T_w - T_{giE}) + h_{1wW} (T_w - T_{giW}) (A_b)}{I_{SE}(t) A_{gE} + I_{SW}(t) A_{gW}} \quad (19)$$

$$\eta_{gth} = \frac{A_b}{P} \left\{ \frac{[h_{1wE} (P - A_2) + h_{1wW} (P - B_2) (T_w)] - [h_{1wE} (A_1) + h_{1wW} (B_1)]}{I_{SE}(t) A_{gE} + I_{SW}(t) A_{gW}} \right\} \quad (20)$$

$$\eta_{gth} = \frac{A_b}{P (I_{SE}(t) A_{gE} + I_{SW}(t) A_{gW})} \left\{ \left[ \frac{h_{1wE} (E_1 - E_2) A_{gE} + h_{1wW} (E'_1 - E'_2) A_{gW}}{2} \right] + \left[ \frac{f_2(t)}{a_2} (1 - e^{-a_2 \Delta t}) + T_{w0} e^{-a_2 \Delta t} \right] - \left[ \frac{K'_{1E} I_{SE}(t) + K'_{1W} I_{SW}(t)}{T_w (H_1 + H_2 + H_3 + H_4)} \right] \right\} \quad (21)$$

Unknown expressions are mentioned in Appendix A: On substituting  $f_2(t)$ ,  $a_2$  in Eq. (21):

$$\eta_{gth} = \frac{A_b}{P} \left( \frac{e^{-a_2 \Delta t}}{I_{SE}(t) A_{gE} + I_{SW}(t) A_{gW}} \right) \left\{ \left[ \frac{h_{1wE} (E_1 - E_2) A_{gE} + h_{1wW} (E'_1 - E'_2) A_{gW}}{H'_{11} + H'_{33}} \right] + \left\{ \left[ \frac{[(\alpha_w + 2\alpha_b h_1) P + K'_{1E}] I_{SE}(t)}{[(\alpha_w + 2\alpha_b h_1) P + K'_{1W}] I_{SW}(t) + D_2 I_C(t)} \right] \right\} (e^{-a_2 \Delta t} - 1) \right\} e^{-a_2 \Delta t} + H'_{11} (T_w - T_a) \quad (22)$$

$$\eta_{gth} = \frac{A_b}{P} \left( \frac{e^{-a_2 \Delta t}}{I_{SE}(t) A_{gE} + I_{SW}(t) A_{gW}} \right) \left\{ \left[ \frac{[(\alpha_w + 2\alpha_b h_1) P + K'_{1E}] I_{SE}(t) + [(\alpha_w + 2\alpha_b h_1) P + K'_{1W}] I_{SW}(t) + D_2 I_C(t)}{(e^{-a_2 \Delta t} - 1) - (K'_{1E} I_{SE}(t) + K'_{1W} I_{SW}(t)) e^{-a_2 \Delta t} + H'_{11} (T_{w0} - T_a)} \right] \right\}$$

$$\eta_{gth} = F' \left[ (\alpha \tau)_{eff} + \frac{(T_{w0} - T_a)}{I_C(t)} (U_{eff}) \right] \quad (23)$$

As an Eq. (23) corresponds to the instantaneous thermal energy efficiency ( $\eta_{gth}$ ) of an active double slope distiller unit with helically coiled heat exchanger (N-PVT-CPC-DS-HE), where

$$H'_{11} = H_1 + H_2 + H_3 + H_4 = U_{eff}$$

$$H'_{33} = U_b A_b - D_1$$

$$Z_{22} = \left[ \frac{h_{1wE} (E_1 - E_2) A_{gE} + h_{1wW} (E'_1 - E'_2) A_{gW}}{H'_{11} + H'_{33}} \right]$$

$$F' = \left( \frac{A_b}{P} \right) e^{-a_2 \Delta t}$$

Table 2  
Thermophysical properties of water (basefluid) [25]

Quality	Symbol	Expression
Density of fluid	$\rho_{bf}$	$999.79 + 0.0683T_{bf} - 0.0107T_{bf}^2 + 0.00082T_{bf}^{2.5} - 2.303 \times 10^{-5}T_{bf}^3$
Specific heat of fluid	$C_{bf}$	$4.2170 - 0.005610T_{bf} - 0.00129T_{bf}^{1.5} + 0.000115T_{bf}^2 - 4.149 \times 10^{-6}T_{bf}^{2.5}$
Viscosity of fluid	$\mu_{bf}$	$\frac{1}{(557.82 - 19.408 \times T_{bf} + 0.136 \times T_{bf}^2 - 3.116 \times 10^{-4} \times T_{bf}^3)}$
Thermal conductivity of fluid	$k_{bf}$	$0.5650 + 0.002630T_{bf} - 0.0001250T_{bf}^{1.5} - 1.5150 \times 10^{-6}T_{bf}^2 - 0.0009410T_{bf}^3$

Table 3  
Thermophysical properties of Al<sub>2</sub>O<sub>3</sub>, TiO<sub>2</sub>, CuO (water based nanofluid) [25–28]

Density	$\rho_{nf} = \varnothing_p \rho_p + (1 - \varnothing_p) \rho_{bf}$
Thermal expansion coefficient	$\beta_{nf} = \varnothing_p \beta_p + (1 - \varnothing_p) \beta_{bf}$
	$k_{nf} = k_{bf} \left[ 1 + (1.01120) \varnothing_p + (2.435) \varnothing_p \left( \frac{47}{d_p (\text{nm})} \right) - (0.02480) \varnothing_p \left( \frac{k_p}{0.613} \right) \right]$ $0 < \varnothing_p < 10\%, 20 < T_{nf} < 70^\circ\text{C}, 11 < d_p < 150 \text{ nm (Al}_2\text{O}_3 - \text{water)}$
	$k_{nf} = k_{bf} \times \left[ 1 + (0.135) \left( \frac{k_{nf}}{k_p} \right)^{0.273} (\varnothing_p)^{0.467} \left( \frac{T_{nf}}{20} \right)^{0.547} \left( \frac{100}{d_p} \right)^{0.234} \right]$
Thermal conductivity	$0 < \varnothing_p < 10\%, 20 < T_{nf} < 70^\circ\text{C}, 11 < d_p < 150 \text{ nm (TiO}_2 - \text{water)}$ $k_{nf} = k_{bf} \times \left[ \begin{aligned} &0.98430 + (0.3980) (\varnothing_p)^{0.4670} \left( \frac{\mu_{nf}}{\mu_{bf}} \right)^{0.0235} \left( \frac{1}{d_p (\text{nm})} \right)^{0.2246} \\ &- (3.9510) \left( \frac{\varnothing_p}{T_{nf}} \right) + (34.0340) \left( \frac{\varnothing_p^2}{T_{nf}} \right) + 32.51 \left( \frac{\varnothing_p}{T_{nf}} \right) \end{aligned} \right]$ $0 < \varnothing_p < 10\%, 20 < T_{nf} < 70^\circ\text{C}, 11 < d_p < 150 \text{ nm (CuO - water)}$
	$\mu_{nf} = -0.4491 + \left( \frac{28.837}{T_{nf}} \right) + 0.547 \varnothing_p - 0.163 (\varnothing_p)^2 + 23.653 \left( \frac{\varnothing_p^2}{d_p^2} \right) + 0.0132 \varnothing_p^3$ $- (2,354.735) \left( \frac{\varnothing_p}{T_{nf}^3} \right) + (23.498) \left( \frac{\varnothing_p^2}{d_p^2} \right) - 3.0185 \left( \frac{\varnothing_p^2}{d_p^2} \right)$ $11 \leq \varnothing_p \leq 9, 13 \leq d_p \leq 130 \text{ nm}, 20 \leq T_{nf} \leq 90^\circ\text{C (Al}_2\text{O}_3 - \text{water)}$
Viscosity	$\mu_{nf} = \mu_{bf} \left[ \left( 1 + \varnothing_p \right)^{11.3} \left( 1 + \frac{T_{nf}}{70} \right)^{-0.038} \left( 1 + \frac{d_p}{70} \right)^{-0.061} \right]$ $10 \leq \varnothing_p \leq 4, 20 \leq d_p \leq 170 \text{ nm}, 0 \leq T_{nf} \leq 70^\circ\text{C (TiO}_2 - \text{water)}$ $\mu_{nf} = (2.414 \times 10^{-5}) \times 10^{\frac{247.8}{(T_{nf} - 140)}}$ $0 \leq \varnothing_p \leq 10, 11 \leq d_p \leq 150 \text{ nm}, 20 \leq T_{nf} \leq 70^\circ\text{C (CuO - water)}$
	$C_{nf} = 0.8429 \left( 1 + \frac{T_{nf}}{50} \right)^{-0.3037} \left( 1 + \frac{\varnothing_p}{100} \right)^{2.272} \left( 1 + \frac{d_p}{50} \right)^{0.4167}$
Specific heat	$15 < d_p < 50 \text{ nm}, 0 < \varnothing_p < 4\%, 20 < T_{nf} < 50^\circ\text{C (Al}_2\text{O}_3 \text{ and CuO - water)}$ $C_{nf} = \left[ A (\varnothing_p)^B (T_{nf})^C \left( \frac{C_p}{C_{p,bf}} \right)^D \right] \times C_{p,bf}$ $A = 1.3870, B = -0.004250, C = 0.001124, D = -0.21159$ $d_p = 21 \text{ nm}, 0 < \varnothing_p < 8\%, 15 < T_{nf} < 65^\circ\text{C (TiO}_2 - \text{water)}$

Table 4  
Coefficients of heat transfer in different areas of the unit (HTCs) [31–36]

Heat transfer coefficients	Relations
Natural convection HTCs of the basin to water	Nusselt number: $(N_u)_w = \frac{(h_{bw})X}{K} = C(R_e P_r)^n$
	Reynolds number: $(R_e)_w = \left(\frac{\rho v X}{\mu}\right)_w$
	$C = 0.540, n = (1/4)$ , plate is horizontally facing uphill From Dunkle’s model
	Evaporation HTCs: $h_{evw} = (0.016273) h_{ef} \left[\frac{P_w - P_{gi}}{T_w - T_{gi}}\right]$
	Convective HTC: $h_{cw} = 0.844 (\Delta T)^{1/3}$
Internal HTC on water surface to inside glass cover	where $P_x = \exp\left[25.17 - \left(\frac{5,144}{T_x}\right)\right]$ ; $\Delta T = [T_w - T_{gi}] + \left[\frac{(P_w - P_{gi})(T_f + 273)}{2.689 \times 10^5 - P_w}\right]$
	Radiative HTC, $h_{rf} = \epsilon_{eff} \sigma [(T_w + 273)^2 + (T_{gi} + 273)^2][T_w - T_{gi} + 546]$
	where $\frac{1}{\epsilon_{eff}} = \frac{1}{\epsilon_w} + \frac{1}{\epsilon_g} - 1$
	Basefluid as water in case I
	$N_u = 1.750 \left(\frac{\mu_{bf}}{\mu_b}\right)^{0.140} \left[Gz_m + 0.0083(Gr_m Pr_m)^{0.75}\right]^{1/3}$
Within compound parabolic (concentrator CPC)	Arithmetic average Graetz number: $Gz_m = \frac{m_f c_{bf}}{k_{bf}^L}$
	Arithmetic average Grashof number: $Gr_m = \frac{g D^2 \Delta T}{\mu_{bf}^b}$
	Here $T$ is bulk temperature difference, $D$ is tube dia., $L$ = length of heated part of tube in nanofluid
	$h_{CPC} = (N_u)_{nf} \frac{k_{nf}}{D_i}$
	$(N_u)_{nf} = \frac{\left(\frac{f}{8}\right) \left((R_e)_{nf} - 10^3\right) (P_r)_{nf}}{1 + 12.7 \sqrt{\frac{f}{8}} \left((P_r)_{nf}^2 - 1\right)}$
For $3 \times 10^3 \leq (R_e)_{nf} \leq 5 \times 10^5$ and $0.55 \leq (P_r)_{nf} \leq 2 \times 10^3$	
$(R_e)_{nf} = \frac{4m_f}{\pi D_i \mu_{nf}}; (P_r)_{nf} = \frac{\mu_{nf} c_{nf}}{k_{nf}}$	
$m_f$ = mass flow rate in any riser $nf$ = darcy friction factor $f = [0.79 \ln(R_e)_{nf} - 1.64]^2$ petukhow correlation for smooth tube Correlations used for tubes roughness	
$\frac{1}{\sqrt{f}} = -2 \log \frac{\epsilon/D_i}{3.7} + \frac{2.51}{(R_e)_{nf} \sqrt{f}}$ for $4 \times 10^3 \leq 5 \times 10^5$ and $\frac{0 < \epsilon}{D_i} < 0.05$	

(Continued)

Table 4 Continued

Heat transfer coefficients	Relations
	$(N_{u'})_{nf} = (2.153 + 0.318(D_e^{0.643})P_r^{0.177})$ For $20 < D_e < 2 \times 10^3$ and $0.7 < P_r < 200$
	Deans number $(D_e)_{nf} = (R_e)_{nf} \sqrt{\frac{d_i}{d_c}}$ ; Reynold number $(R_e)_{nf} = \frac{4m_f}{\pi D_i \mu_{nf}}$
	$d_c = \text{coil diameter}; d_i = r_{11} \text{ innertube diameter}$ $(N_{u'})_{nf} = 3.67(D_e^{0.67}\delta^{0.009}\phi^{1.004})$
	$h_{nf} = \frac{(N_{u'})_{nf} k_{eff}}{d_i}; k_{eff} = k_{static} + k_{brownian}$
Within heat exchanger	$k_{static} = \left[ \frac{k_{np} + 2k_{bf} - 2\phi(k_{bf} - k_{np})}{k_{np} + 2k_{bf} + \phi(k_{bf} - k_{np})} \right]$ and
	$k_{static} = (5 \times 10^4) \left[ \beta \phi \rho_{nf} c_{bf} \sqrt{\frac{k_b T}{2\rho_{np} R_{np}}} \right], f(T, \phi)$
	$\beta = 8.44 \times 100 \times \phi e^{-1.07304}$ for $1 \leq \phi \leq 10\%$ ( $Al_2O_3$ nanoparticle)
	Function of modeling:
	$f(T, \phi) = (2.820 \times 10^{-2} \phi + 3.910 \times 10^{-3}) \left( \frac{T}{T_0} \right) - (3.069 \times 10^{-2} \phi + 3.91 \times 10^{-3})$
	where, $\phi = \text{nanoparticles concentrations};$ and $\delta = d_i/d_c, T_0 = \text{reference temperature}$

Table 5

Enhancement in average daily yield, average thermal energy and average thermal exergy of proposed system over the previous research

Parameters	Thermal energy, exergy and daily yield			Enhancement (%)		
	Thermal energy (kW/m <sup>2</sup> )	Thermal exergy (kW/m <sup>2</sup> )	Daily yield (kg)	Thermal energy	Thermal exergy	Daily yield (kg)
Proposed system	165.13	1.31	10.56	13.68	8.22	16.31
Previous research	145.25	1.21	9.08			

$$(\alpha\tau)_{eff} = \left[ \frac{1}{(I_{SE}(t)A_{gE} + I_{SW}(t)A_{gW})} \right] \left\{ z_{22} \left\{ \left[ \begin{aligned} &[(\alpha_w + 2\alpha_b h_1)P + K'_{1E}]I_{SE}(t) + \\ &[(\alpha_w + 2\alpha_b h_1)P + K'_{1W}]I_{SW}(t) + \\ &D_2 I_C(t)(e^{-a_2 \Delta t} - 1) \\ &-(K'_{1E} I_{SE}(t) + K'_{1W} I_{SW}(t))e^{-a_2 \Delta t} \end{aligned} \right] \right\} \right\}$$

Later an equation for the instantaneous loss thermal energy efficiency can be calculated by substituting the equation.

$$\frac{dT_w}{dt} + a_2 T_w = f_2(t)$$

In the equation:

$$\eta_{Lth} = \frac{m_f C_f (T_w - T_{w0})}{(I_{SE}(t)A_{gE} + I_{SW}(t)A_{gW})}$$

$$\eta_{Lth} = \left( \frac{m_f C_f}{(I_{SE}(t)A_{gE} + I_{SW}(t)A_{gW})} \right) \left( \frac{1}{(H'_{11} + H'_{33})} \right) \left\{ \left[ \begin{aligned} &[(\alpha_w + 2\alpha_b h_1)P + K'_{1E}]I_{SE}(t) + [(\alpha_w + 2\alpha_b h_1)P + K'_{1W}] \\ &I_{SW}(t) + D_2 I_C(t)(1 - e^{-a_2 \Delta t}) + (H'_{11} + H'_{33})(T_{w0} - T_a)(e^{-a_2 \Delta t} - 1) \end{aligned} \right] \right\} \quad (24)$$

$$\eta_{Lth} = F'_L \left[ (\alpha\tau)_{Leff} - U'_{Leff} \frac{(T_{w0} - T_a)}{I(t)} \right] \quad (25)$$

where

$$F'_L = \frac{m_f C_f}{(H'_{11} + H'_{33})}$$

$$(\alpha\tau)_{\text{Leff}} = [(\alpha_w + 2\alpha_b h_1)P + K'_{1E}]I_{\text{SE}}(t) + [(\alpha_w + 2\alpha_b h_1)P + K'_{1w}]I_{\text{SW}}(t) + D_2 I_C(t) (1 - e^{-a_2 \Delta t})$$

$$U'_{\text{Leff}} = (H'_{11} + H'_{33})(e^{-a_2 \Delta t} - 1)$$

$$H'_{33} = U_b A_b - D_1$$

On the basis of the thermodynamics laws for the given entities, the analysis of energy and exergy has been done, respectively. Per hour variation in thermal energy ( $E_{\text{hourlyEn}}$ ) and exergy ( $E_{\text{hourlyEx}}$ ) of proposed system can be taken using following relations [37,38].

$$E_{\text{hourlyEn}} = [h_{1wE}(T_w - T_{\text{giE}}) + h_{1wW}(T_w - T_{\text{giW}})](A_b) \tag{26}$$

$$E_{\text{hourlyEx}} = \left\{ \begin{aligned} &h_{1wE} \left[ (T_w - T_{\text{giE}}) - (T_a + 273) \ln \left( \frac{T_w + 273}{T_{\text{giE}} + 273} \right) \right] + \\ &h_{1wW} \left[ (T_w - T_{\text{giW}}) - (T_a + 273) \ln \left( \frac{T_w + 273}{T_{\text{giW}} + 273} \right) \right] \end{aligned} \right\} A_b \tag{27}$$

$$\eta_{\text{hourlyEn}} = \left\{ \frac{M_w \times L_v}{A_c \times I_c(t) + A_s I_s(t) \times 3,600} \right\} \times 100 \tag{28}$$

$$\eta_{\text{hourlyEx}} = \left( \frac{100}{0.933 \times A_s \times I_s(t)} \right) \times \left\{ \begin{aligned} &h_{1wE} \left[ (T_w - T_{\text{giE}}) - (T_a + 273) \ln \left( \frac{T_w + 273}{T_{\text{giE}} + 273} \right) \right] + \\ &h_{1wW} \left[ (T_w - T_{\text{giW}}) - (T_a + 273) \ln \left( \frac{T_w + 273}{T_{\text{giW}} + 273} \right) \right] \end{aligned} \right\} A_b \tag{29}$$

The constant 0.933 expresses the exchange constant for solar radiation of exergy, per hour water generation of the proposed system that can calculate by the mentioned equation.

$$M_w = \frac{q_{\text{ew}}}{L_v} \times 3,600 = \frac{h_{\text{ew}}(T_w - T_g)}{L_v} \times 3,600 \tag{30}$$

where the latent heat of vaporization is expressed as [38]:

$$\begin{aligned} L_v &= 3.1625 \times 10^6 + [1 - (7.616 \times 10^{-4} \times T_v)] \text{ for } T_v > 70^\circ\text{C} \\ L_v &= 2.4935 \times 10^6 \times [1 - (9.4779 \times 10^{-4} \times T_v) + 1.3132 \times 10^{-7} \times (T_v^2) - 4.7974 \times 10^{-3}(T_v^3)] \\ &\text{For } T_v < 70^\circ\text{C} \end{aligned}$$

Hourly change in basal water temperatures [Eq. (17)], thermal energy [Eq. (26)], thermal exergy [Eq. (27)], and output [Eq. (30)] of the proposed water system loaded

nanoparticles have been obtained using thermal transfer relationships [10,19], relationship for thermophysical properties of vapor, basefluid [25–28] and nanoparticles (Table 4) [31–36].

#### 4. Methodology

In the present paper, the annual number of days for climatic conditions of (a), (b), (c), and (d) for New Delhi is taken, and entities have been extracted out from IMD, Pune, India. Using Liu and Jordan formula, sun radiation on the cover of toughened glass inclined at 30° of double slope helically coiled heat exchanger solar still and inclination 45° opted for partly covered photovoltaic thermal (N-PVT-CPC-DS-HE) compound parabolic concentrator is calculated with the help of MATLAB-R2016a [52]. The variations of sun radiant energy and temperature of ambient are annually shown in Figs. 4 and 5. The procedure adopted to study the proposed system (CuO water-based nanoparticles) is performed by using a characteristic curve for collectors  $N = 4$ , for flow rate of 0.02 kg/s, 280 kg basin fluid 0.25% concentration of metallic nanoparticles.

For better understanding the methodology for numerical computation of N-PVT-FPC-DS-HE/N-PVT-CPC-DS-HE and their subsequent comparison, a flow chart has been drawn as follows. Fig. 3 represents the flow chart for a better understanding of the methodology followed for carrying out analysis.:

##### Step I

The initial values of temperature of the heat exchanger, basin fluid temperature, input and output temperature of collector, etc., are taken equal to ambient temperature. Based on the initial input, using properties of thermo-physical for basefluid from Table 2 and CuO-nanoparticles from Table 3, the output temperatures have been calculated. The relevant equations have been used to assess the temperature of water of double slope solar still [Eq. (18)], collector outlet fluid temp [Eq. (11)], and fluid temp in the heat exchanger [Eq. (10)].

##### Step II

The coefficients of collectors of double slope distiller unit using a helically coiled heat exchanger (N-PVT-CPC-DS-HE) and internal heat transfer coefficient have been calculated and compared by using relations as given in Table 4.

##### Step III

Eqs. (26), (27) and (30) have been used for thermal energy, thermal exergy, and productivity, respectively, and results are compared for the mass of 100 and 280 kg of basin fluid.

#### 5. Result and discussion

Hourly variation of temperature in different sections of Nth double slope photovoltaic compound parabolic concentrator collector with helically coiled heat exchanger (N-PVT-CPC-DS-HE) proposed system and (N-PVT-FPC-DS-HE) previous system both systems are presented in Figs. 1 and 2. In these systems, the different temperatures

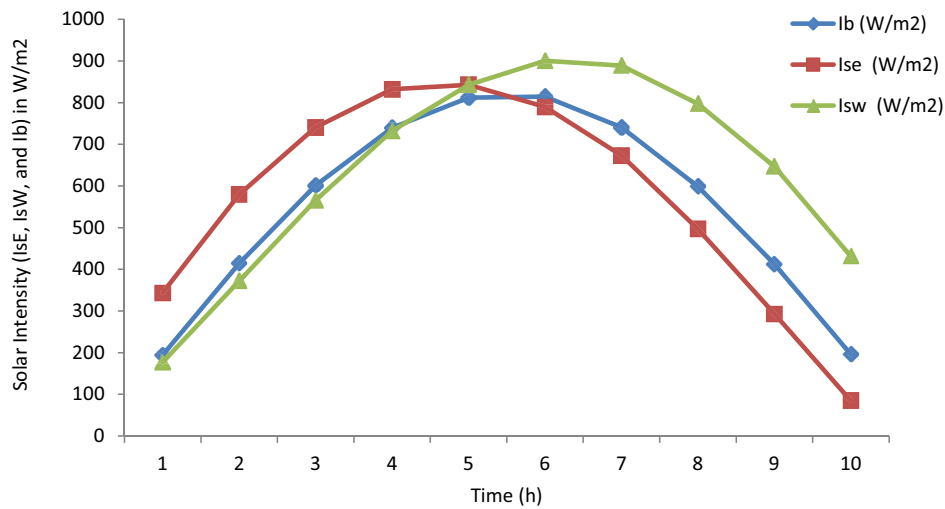


Fig. 4. Hourly variation of solar intensity for New Delhi climatic conditions.

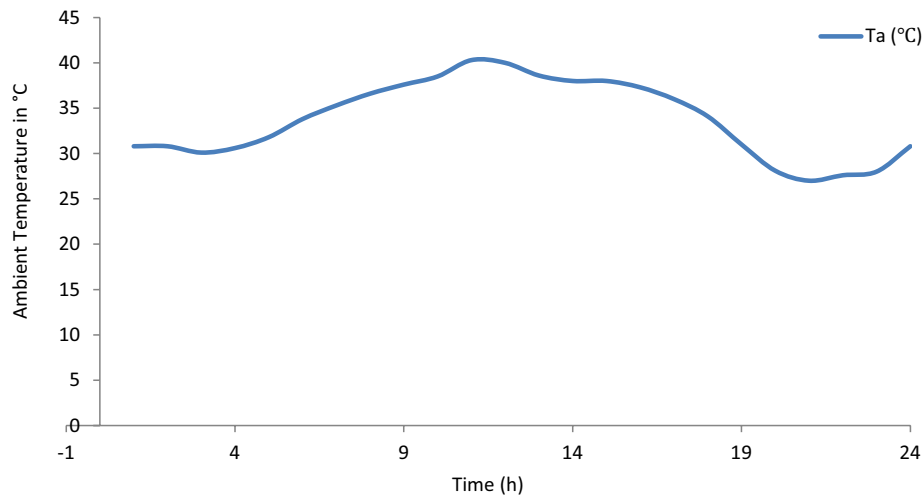


Fig. 5. Hourly variation of ambient temperature on a typical day of the month of May in New Delhi.

of the proposed system are found to be higher in comparison to the previous system.

Fig. 6 shows the positive increment in basin water temperature for the proposed system by  $5.97^{\circ}\text{C}/\text{d}$  for the same basin area compared to the previous research. The increasing trend of graph continuous up to May and the gap between the proposed and existing work is almost uniform. Hence, the influence of CuO-nanoparticles in the helically coiled heat exchanger increases the temperature and conducts through it the basin water in an efficient manner. The average temperature daily for the proposed system is extensively enhanced than the previous system, that is,  $47.30$  and  $42.99^{\circ}\text{C}/\text{d}$ , respectively. The higher temperature is due to external thermal energy from PVT-CPC.

Fig. 7 shows the affirmative growth in the inside glass temperature of Eastside for the proposed system by  $4.37^{\circ}\text{C}/\text{d}$  for the same basin area compared to the previous research. The increasing trend of the graph is continuous up to May, and the generalized gap between proposed and existing work is almost uniform. Hence, the influence of

CuO-nanoparticles in the helically coiled heat exchanger increases the temperature and conducts the basin water efficiently. The average temperature daily for the proposed unit is extensively enhanced than the already existing system, and results appear as:  $40.02$  and  $37.24^{\circ}\text{C}/\text{d}$ , respectively.

Fig. 8 shows the affirmative growth in the inside glass temperature of the west side for the proposed system by  $4.37^{\circ}\text{C}/\text{d}$  for the same basin area is compared to previous research. The increasing trend of the graph is continuous up to May, and the generalized gap between proposed and existing work is almost uniform. Hence, the influence of CuO-nanoparticles in the helically coiled heat exchanger increases the temperature and conducts the basin water efficiently. The average temperature daily for the proposed system is extensively enhanced than the already existing unit, and results appear as:  $39.96$  and  $37.23^{\circ}\text{C}/\text{d}$ , respectively.

Fig. 9 shows the optimistic addition in heat energy on the east side for the proposed system ( $22.99 \text{ kW}/\text{m}^2/\text{d}$ ) compared to the earlier research for the same basin area. The increasing trend of the graph is continuous up

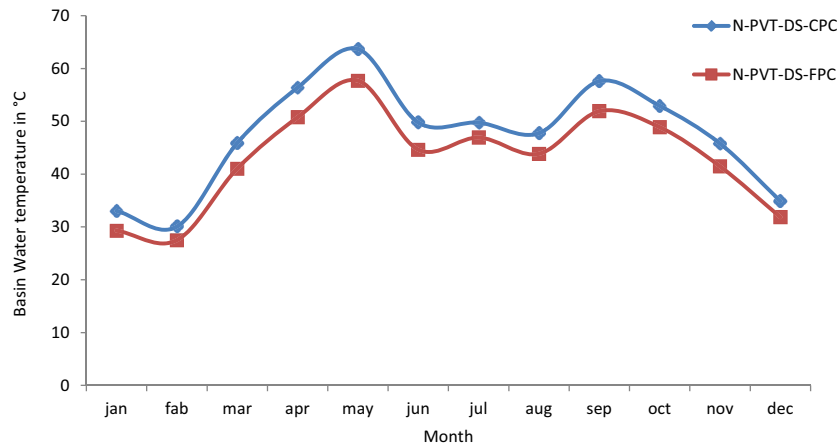


Fig. 6. Monthly variation in temperature of basin water in (°C).

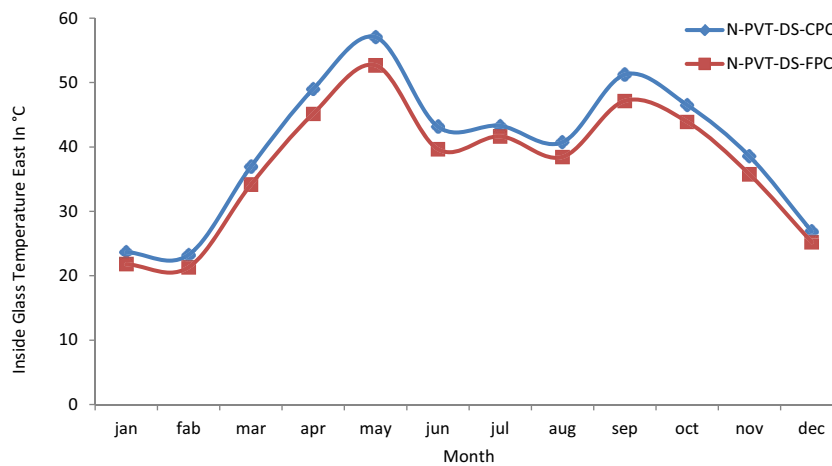


Fig. 7. Monthly variation in inside glass temperature East-side (°C).

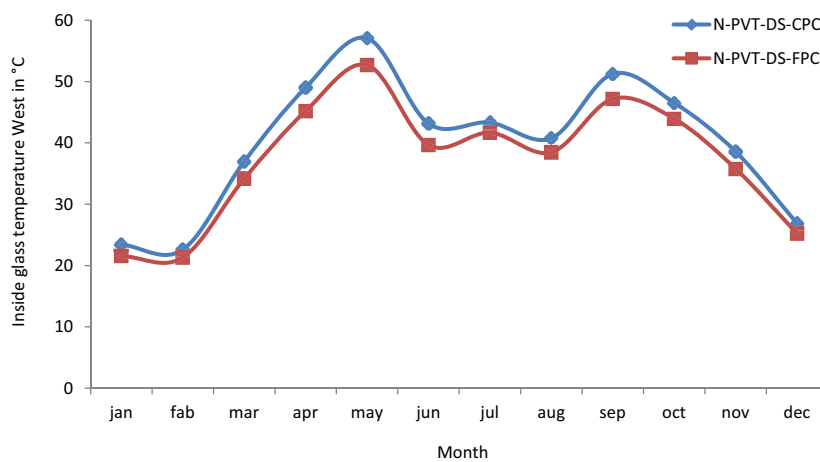


Fig. 8. Monthly variation in inside glass temperature West-side (°C).

to May, and the generalized gap between proposed and existing work is almost uniform. Hence, the influence of CuO-nanoparticles in the helically coiled heat exchanger increases the temperature and conducts through it the

basin water in an efficient manner. The average heat energy daily for the proposed system is extensively enhanced than the already existing unit, and results appear as: 165.7 and 145.7 kW/m<sup>2</sup>/d correspondingly.

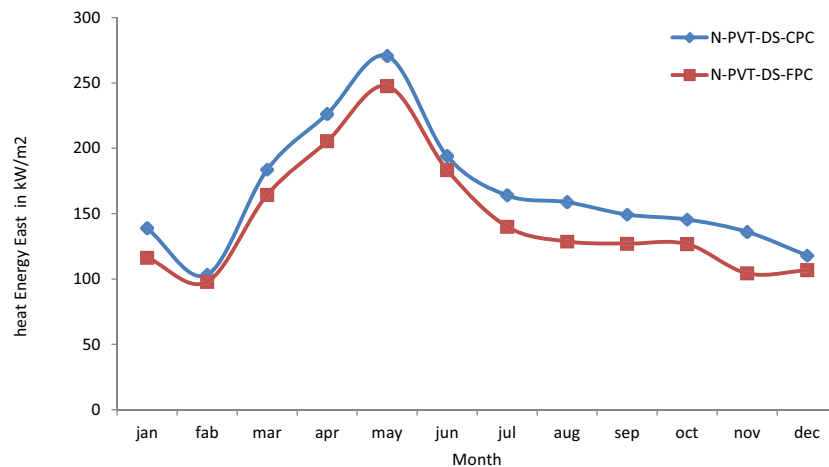


Fig. 9. Monthly variation of heat energy in kW/m<sup>2</sup> (East-side).

Fig. 10 shows the optimistic addition in heat energy on the west side for the proposed system (22.95 kW/m<sup>2</sup>/d) compared to the earlier research for the same basin area. The increasing trend of the graph continuous up to May and the generalized gap between proposed and existing work is almost uniform. Hence, the influence of CuO-nanoparticles in the helically coiled heat exchanger increases the temperature and conducts through it the basin water in an efficient manner. The average heat energy daily for the proposed system is extensively enhanced than the already existing unit, and results appear as: 164.56 and 144.75 kW/m<sup>2</sup>/d respectively.

Fig. 11 shows the constructive augmentation in heat transfer coefficient on the east side for the proposed system by 17.32 W/m<sup>2</sup>°C/d for the same basin area compared to the previous research. The increasing trend of the graph continuous up to May and the generalized gap between proposed and existing work is almost uniform. Hence, the influence of CuO-nanoparticles in the helically coiled heat exchanger increases the temperature and conducts through it the basin water in an efficient manner. The average heat transfer coefficient temperature daily for the proposed system is extensively enhanced than the already

existing unit, and results appear as 37.52 and 30.54 W/m<sup>2</sup>°C/d correspondingly.

Fig. 12 shows the constructive augmentation in heat transfer coefficient on the west side for the proposed system by 17.31 W/m<sup>2</sup>°C/d for the same basin area is compared to the previous researcher. The increasing trend of the graph continuous up to May and the generalized gap between proposed and existing work is almost uniform. Hence, the influence of CuO-nanoparticles in the helically coiled heat exchanger increases the temperature and conducts through it the basin water in an efficient manner. The average heat transfer coefficient basis for the proposed unit is extensively enhanced than the already existing unit, and results appear as: 37.47 and 30.49 W/m<sup>2</sup>°C/d correspondingly.

Fig. 13 shows the electrical exergy for the proposed system at 11.22, 12.38 and 12.08 kWh/month for the same basin area compared to the previous research. With the increasing trend of the graph for the month, the generalized gap between proposed and existing work is almost uniform. Hence it can be predicted that the influence of CuO-nanoparticles in the helically coiled heat exchanger does not affect electricity generation due to photovoltaic thermal attached to the system. The average electrical

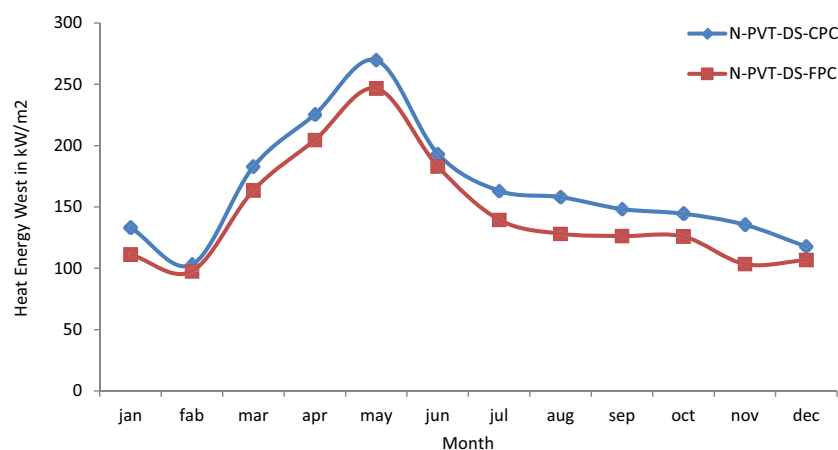


Fig. 10. Monthly variation of heat energy in kW/m<sup>2</sup> (West-side).

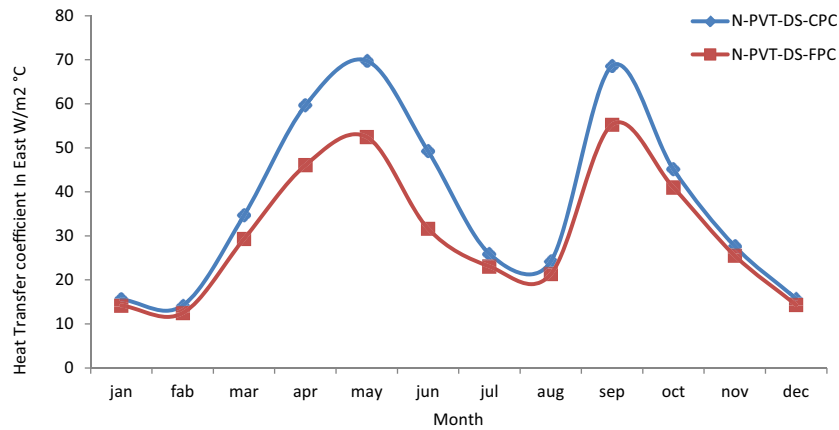


Fig. 11. Monthly variation in heat transfer coefficient (East-side).

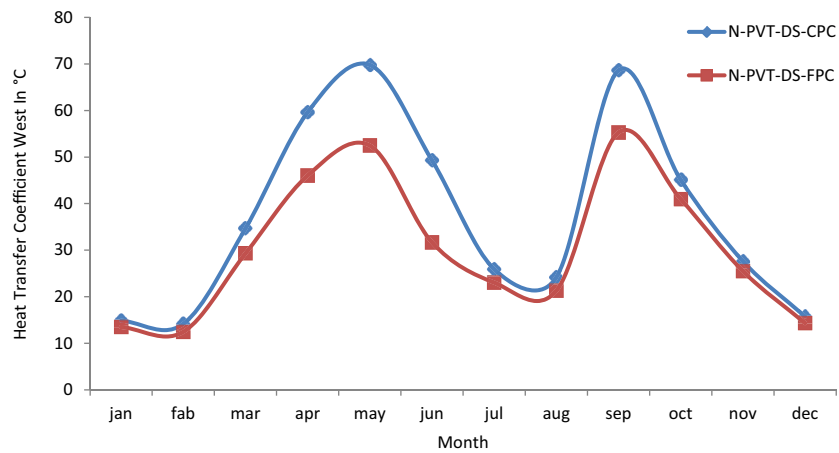


Fig. 12. Monthly variation in heat transfer coefficient (West-side).

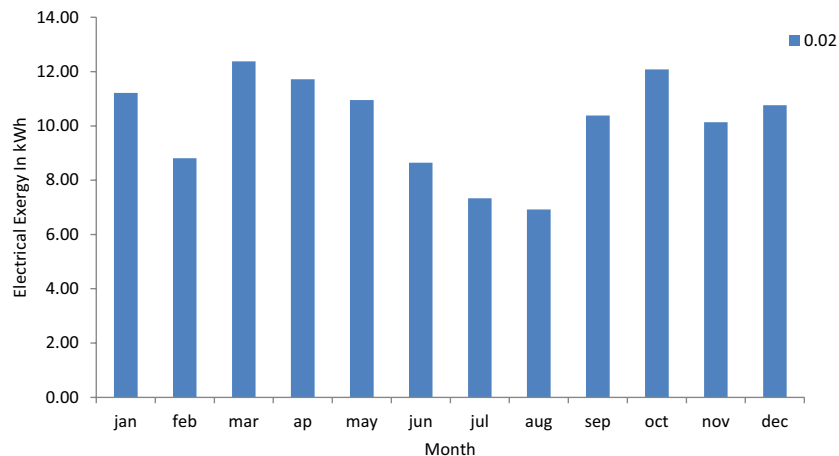


Fig. 13. Mean electrical exergy in kWh/month.

exergy daily for the proposed system is significantly higher than the already existing system, and the results appear-as: 11.22, 12.38, and 12.08 kWh/month 12.38 kWh/month (maximum) and 6.93 kWh/month (minimum), which depend on the covering of the photovoltaic thermal system, which

is 25% in the previous and the proposed system. These results can be further improved by increasing the coverage area by 50%, 75%, and 100%. The proposed system can generate a sufficient amount of electricity used to operate the pump’s motor to circulate water, and the rest can

be stored for further use when there is no sunlight. So this system is called self-sustainable.

Fig. 14 shows the positive increment in thermal exergy for the proposed system (0.16 kWh/d) for the same basin area compared to the previous research. The increasing trend of the graph continuous up to May and the generalized gap between proposed and existing work is almost uniform. Hence, it can be predicted that the influence of CuO-nanoparticles in the helically coiled heat exchanger increases the temperature and conducts through it the basin water in an efficient manner. The average thermal exergy daily for the proposed unit is extensively enhanced than the already existing unit, and results appear as: 1.31 and 1.22 kWh/d, respectively.

Fig. 15 shows the positive increment in daily yield for the proposed system by 2.43 kg/d for the same basin area compared to the previous research. The increasing trend of the graph continuous up to May and the generalized gap between proposed and existing work is almost uniform. Hence, it can be predicted that the influence of CuO-nanoparticles in the helically coiled heat exchanger increases the temperature and conducts through it the basin water in an efficient manner. The average yield daily for the proposed

unit is extensively enhanced than the already existing unit, and results appear as: 10.56 and 9.08 kg/d, respectively.

As the previous research has low value of yield, thermal energy and thermal exergy in case of FPC while the proposed research has CPC there is a countable increment in yield, thermal energy and thermal exergy respectively. Remarkable enhancement is seen.

## 6. Conclusions

The performance of the proposed system and the previous system has been studied using characteristic equations and analyzed the effect of using CuO-nanoparticles and found better performance over the previous studies. In a study of both systems, it is found that the performance of the proposed system is better than the previous system. The performance observed based on maximum temperature difference, thermal energy, thermal exergy, heat transfer coefficients, and generation of potable water is found to be greater using N-PVT-CPC-DS-HE using CuO-nanoparticles. The utilization of CPC further increases the water temperature up east and west side up to max. 4.37°C and min. 1.64°C. The 25% covered PVT produces 97.6% excess electricity that

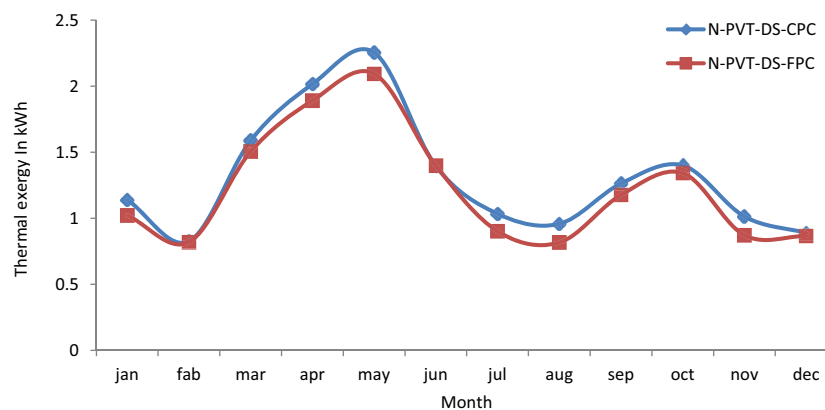


Fig. 14. Monthly average variation in thermal exergy in kWh.

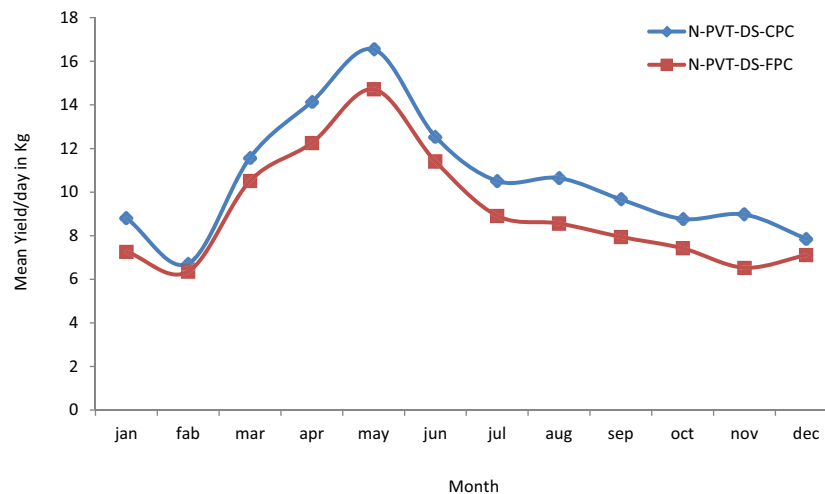


Fig. 15. Daily yield in kg of the proposed system.

can be utilized for other supportive applications. The optimum mass flow rate achieved is 0.02 kg/s than the previous 0.03 kg/s, that is, decreased about 33%. This decrement in mass flow rate will also improve the pump performance and reduce the maintenance required for the pump.

**Future scope**

The present work can be further expanded by doing intensive research in CPC-PVT-PCM utilizations up to their optimum level. The partly covered FPC can be increased beyond 25% to run the system at night with additional supportive electrical subsystems. The profile of CPC may further increase the mass water temperature and can be further utilized by the PCM at night. It can be another cause for the system performance enhancement, and to quantify that, further research is needed.

**Symbols**

- $A_b$  — Basin region, m<sup>2</sup>
- $A_c$  — Under glazing region of collector, m<sup>2</sup>
- $A_{gE}$  — East side glass cover area, m<sup>2</sup>
- $A_{gW}$  — West side glass cover area, m<sup>2</sup>
- $A_m$  — PVT area, m<sup>2</sup>
- $a$  — Blue sky (clear days)
- $b$  — Hazy days
- $C_p$  — Heat nanoparticle (specific in J/kg-K)
- $C_{bf}$  — Basefluid heat (specific in J/kg-K)
- $C_{nf}$  — Heat nanofluid (specific in J/kg-K)
- $D_i$  — Collector tube dia. in m
- $d_p$  — Nanoparticle dia. in nm
- CPC — Compound parabolic concentrator
- $c$  — Partially foggy and unclear days
- $d$  — Fully unclear days
- DS — Distiller unit with double slope
- $F'$  — Collector efficiency factor
- $h_i$  — Coefficient of heat transfer glazing and absorbing plate, W/m<sup>2</sup> K
- $h_0$  — Coefficient of heat transfer PVT to ambient, W/m<sup>2</sup> K
- $h_{pw}$  — Coefficient of heat transfer blackened plate to fluid, W/m<sup>2</sup> K
- $h_{bw}$  — Coefficient of heat transfer basin liner to water, W/m<sup>2</sup> K
- $h_{ba}$  — Coefficient of heat transfer basin liner to ambient, W/m<sup>2</sup> K
- $h_{CPC}$  — Coefficient of convective heat transfer, at CPC, W/m<sup>2</sup> K
- $h_{HE}$  — Coefficient of convective heat transfer, in heat exchanger, W/m<sup>2</sup> K
- $h_{rwgE}$  — Coefficient of radiant heat transfer water surface to inside of glass cover in east, W/m<sup>2</sup> K
- $h_{rwgW}$  — Coefficient of radiant heat transfer water surface to inside of glass cover in west, W/m<sup>2</sup> K
- $h_{cwgE}$  — Coefficient of convective heat transfer, surface water to inside glass cover in east, W/m<sup>2</sup> K
- $h_{cwgW}$  — Coefficient of heat transfer convective, water surface to inside of glass cover in west, W/m<sup>2</sup> K
- $h_{ewgE}$  — Coefficient of heat transfer evaporative, water surface to inside of glass cover in east, W/m<sup>2</sup> K
- $h_{ewgW}$  — Coefficient of heat transfer evaporative, water surface to inside of glass cover in west, W/m<sup>2</sup> K

- $h_{1gE}$  — Coefficient of total heat transfer in east, W/m<sup>2</sup> K
- $h_{1gW}$  — Coefficient of total heat transfer in west, W/m<sup>2</sup> K
- $h_{1wE}$  — Coefficient of total heat transfer amid fluid area and glass cover in east, W/m<sup>2</sup> K
- $h_{1wW}$  — Coefficient of total heat transfer amid fluid area and glass cover in west, W/m<sup>2</sup> K
- $I_b$  — Radiant energy falls on collector, W/m<sup>2</sup>
- $I_{sE}$  — Radiant energy falls on glass cover in east, W/m<sup>2</sup>
- $I_{sW}$  — Radiant energy falls on glass cover in west, W/m<sup>2</sup>
- $K_g$  — Glass thermal conductivity, W/m K
- $K_i$  — Insulation thermal conductivity, W/m K
- $K_p$  — Absorption plate thermal conductivity, W/m K
- $k_p$  — Nanoparticle thermal conductivity, W/m K
- $K_{nf}$  — Nanoparticle thermal conductivity, W/m K
- $k_{bf}$  — Basefluid thermal conductivity, W/m K
- $L$  — Helical coiled heat exchanger length, m
- $L_c$  — Under glazing collector length, m
- $L_i$  — Insulation thickness, m
- $L_g$  — Glass cover thickness, m
- $L_m$  — PV module length, m
- $L_p$  — Absorption plate thickness, m
- $M_w$  — Mass of basin water, kg
- $M_{ew}$  — Per annum water generation, kg
- $m_f$  — Flow rate of water, Kg/s
- PVT — Photovoltaic thermal
- PF<sub>1</sub> — Penalty factor by glass cover module
- PF<sub>2</sub> — Penalty element with a suction plate under the module
- PF<sub>3</sub> — Penalty element with a suction plate on the polished assignment
- PF<sub>c</sub> — Penalty factor by glass covers to glazed portion
- $P_{gi}$  — Partially pressure of saturated vapor of glass cover, N/m<sup>2</sup>
- $r_{11}$  — Outside dia. of helical coiled heat exchanger, m
- $r_{22}$  — Inside dia. of the helical coiled heat exchanger, m
- $T_{giE}$  — Temperature inside glass cover of solar distiller in east, °C
- $T_{giW}$  — Temperature of inner glass cover of solar distiller in west °C
- $T_{goE}$  — Temperature outside glass cover of solar distiller in east, °C
- $T_{goW}$  — Temperature of outside glass cover of solar distiller in west, °C
- N-PVT-CPC-DS — Nth serially connected PVT-CPC double slope solar distiller unit
- $Q_{uN}$  — Usable heat to N alike partly covered PVT-CPC, kWh

$R$	—	Reflectivity
$r$	—	Fraction of per day diffused to per day total radiation
$T_a$	—	Ambient temperature, °C
$T_c$	—	Solar cell temperature, °C
$T_{cN}$	—	Average solar cell temperature, °C
$T_{wi}$	—	Input water temperature of collector, °C
$T_{bf}$	—	Temperature of basefluid in collector, °C
$T_{woN}$	—	Output water temperature of collector, °C
$T_{nf}$	—	Nanoparticle temperature, °C
$T_p$	—	Temperature of absorption plate, °C
$T_s$	—	Temperature of sun, °C
$T_v$	—	Vapor temperature, °C
$T_w$	—	Temperature in basin water, °C
$T_{wo}$	—	Temperature of water, °C at $t = 0$
$\Delta T_{DSSS}$	—	Temperature difference amid nanoparticle to basefluid in distiller unit, °C
$\Delta T_{CPC}$	—	Temperature difference amid nanoparticle to basefluid at the output of PVT collector, °C
$\Delta T_{HE}$	—	Temperature difference amid nanoparticle to basefluid in heat exchanger, °C
$U_{tca}$	—	Total heat transfer coefficient, cell to ambient, $W/m^2 K$
$U_{tpa}$	—	Total heat transfer coefficient, suction plate to ambient, $W/m^2 K$
$U_{lm}$	—	Total heat transfer coefficient, PV module to ambient, $W/m^2 K$
$U_{lc}$	—	Total heat transfer coefficient, glazing to ambient, $W/m^2 K$
$U_{ga}$	—	Coefficient of total heat transfer, condensing cover to ambient, $W/m^2 K$
$U_{ba}$	—	Total heat transfer coefficient, base liner to ambient, $W/m^2 K$
$U_{gaE}$	—	Total heat transfer coefficient, condensing cover of east side to ambient, $W/m^2 K$
$U_{gaW}$	—	Total heat transfer coefficient, condensing cover of west side to ambient, $W/m^2 K$
$U_{tc,p}$	—	Total heat transfer coefficient, cell to absorption plate, $W/m^2 K$
$X$	—	Characteristic length of solar distiller unit, m

### Greek

$\alpha_g$	—	Condensing cover absorbed solar radiation
$\alpha_b$	—	Basin surface absorbed solar radiation
$\alpha_f$	—	Water absorbed solar radiation
$\alpha_c$	—	Solar cell absorbed solar radiation
$\tau_g$	—	Top glass cover transmitted solar radiation
$\phi_g$	—	Volume fraction of NPs, %
$\eta_g$	—	Collector efficiency, %
$\beta$	—	Packing factor
$\beta_p$	—	Coefficient of thermal expansion of nanoparticle, $K^{-1}$
$\beta_{nf}$	—	Coefficient of thermal expansion of nanofluid, $K^{-1}$
$\beta_{bf}$	—	Coefficient of thermal expansion of basefluid, $K^{-1}$
$\mu_{bf}$	—	Basefluid dynamic viscosity, $Ns/m^2$
$\mu_{nf}$	—	Nanofluid dynamic viscosity, $Ns/m^2$
$\rho_p$	—	Nanoparticle density, $kg/m^3$
$\rho_{nf}$	—	Nanofluid density, $kg/m^3$
$\rho_{bf}$	—	Basefluid density, $kg/m^3$

### Subscripts

$a$	—	Ambient air
$b$	—	Basin area
$v$	—	Vapour
$g_i$	—	Inside condensing cover
$g_o$	—	Outside condensing cover
$w$	—	Water (fluid)
$p$	—	Particles
CPC	—	Compound parabolic concentrator
th	—	Thermal
sol	—	Solar
$E$	—	Eastern side
$W$	—	Western side
ann	—	Per annum
ex	—	Exergy
en	—	Energy

### Abbreviation

HTC	—	Factor of heat transfer coefficient
DSSS	—	Solar distiller unit of double slope
CPC	—	Compound parabolic concentrator
NPs	—	Nanoparticles
HE	—	Heat exchanging device
NF	—	Mixture of nanoparticle and glycol
BF	—	Basefluid

### References

- [1] E. Delyannis, Historic background of desalination and renewable energies, *Sol. Energy*, 75 (2003) 357–366.
- [2] G.N. Tiwari, H.N. Singh, R. Tripathi, Present status of solar distillation, *Sol. Energy*, 75 (2003) 367–373.
- [3] R. Dev, G.N. Tiwari, Characteristic equation of a passive solar still, *Desalination*, 245 (2009) 246–265.
- [4] R. Dev, H.N. Singh, G.N. Tiwari, Characteristic equation of double slope passive solar still, *Desalination*, 267 (2011) 261–266.
- [5] R. Dev, G.N. Tiwari, Characteristic equation of the inverted absorber solar still, *Desalination*, 269 (2011) 67–77.
- [6] R. Dev, G.N. Tiwari, Characteristic equation of a hybrid (PV-T) active solar still, *Desalination*, 254 (2010) 126–137.
- [7] R. Dev, S.A. Abdul-Wahab, G.N. Tiwari, Performance study of the inverted absorber solar still with water depth and total dissolved solid, *Appl. Energy*, 88 (2011) 252–264.
- [8] H.S. Soliman, Solar still coupled with a solar water heater, Mosul University, Mosul, Iraq, 1976.
- [9] S.N. Rai, G.N. Tiwari, Single basin solar still coupled with flat plate collector, *Energy Convers. Manage.*, 23 (1983) 145–149.
- [10] S.A. Lawrence, G.N. Tiwari, Theoretical evaluation of solar distillation under natural circulation with heat exchanger, *Energy Convers. Manage.*, 30 (1990) 205–213.
- [11] S. Kumar, G.N. Tiwari, Optimization of daily yield for an active double effect distillation with water flow, *Energy Convers. Manage.*, 40 (1999) 703–715.
- [12] M.K. Gaur, G.N. Tiwari, Optimization of number of collectors for integrated PV/T hybrid active solar still, *Appl. Energy*, 87 (2010) 1763–1772.
- [13] Shyam, G.N. Tiwari, I.M. Al-Helal, Analytical expression of temperature dependent electrical efficiency of N-PVT water collectors connected in series, *Sol. Energy*, 114 (2015) 61–76.
- [14] Shyam, G.N. Tiwari, O. Fischer, R.K. Mishra, I.M. Al-Helal, Performance evaluation of N-photovoltaic thermal (PVT) water collectors partially covered by photovoltaic module connected in series: an experimental study, *Sol. Energy*, 130 (2016) 302–313.
- [15] M. Boukar, A. Harmim, Performance evaluation of a one-sided vertical solar still tested in the desert of Algeria, *Desalination*, 183 (2005) 113–126.

- [16] R. Dev, G.N. Tiwari, Annual performance of evacuated tubular collector integrated solar still, *Desal. Water Treat.*, 41 (2012) 204–223.
- [17] G.N. Tiwari, L. Sahota, Review on the energy and economic efficiencies of passive and active solar distillation systems, *Desalination*, 401 (2017) 151–179.
- [18] M.A. Khairul, R. Saidur, M.M. Rahman, M.A. Alim, A. Hossain, Z. Abidin, Heat transfer and thermodynamic analyses of a helically coiled heat exchanger using different types of nanofluids, *Int. J. Heat Mass Transfer*, 67 (2013) 398–403.
- [19] O. Mahian, A. Kianifar, A.Z. Sahin, S. Wongwises, Performance analysis of a minichannel-based solar collector using different nanofluids, *Energy Convers. Manage.*, 88 (2014) 129–138.
- [20] A. Mwesigye, Z. Huan, J.P. Meyer, Thermal performance and entropy generation analysis of a high concentration ratio parabolic trough solar collector with Cu-Therminol@VP-1 nanofluid, *Energy Convers. Manage.*, 120 (2016) 449–465.
- [21] R. Tripathi, G.N. Tiwari, Energetic and exergetic analysis of  $N$  partially covered photovoltaic thermal-compound parabolic concentrator (PVT-CPC) collectors connected in series, *Sol. Energy*, 137 (2016) 441–451.
- [22] D. Atheaya, A. Tiwari, G.N. Tiwari, I.M. Al-Helal, Analytical characteristic equation for partially covered photovoltaic thermal (PVT) compound parabolic concentrator (CPC), *Sol. Energy*, 111 (2015) 176–185.
- [23] Dharamveer, Samsher, D.B. Singh, A.K. Singh, N. Kumar, Solar Distiller Unit Loaded with Nanofluid—A Short Review, M. Kumar, R. Pandey, V. Kumar, Eds., *Advances in Interdisciplinary Engineering, Lecture Notes in Mechanical Engineering*, Springer, Singapore, 2019, pp. 241–247.
- [24] S. Dubey, G.N. Tiwari, Analysis of PV/T flat plate water collectors connected in series, *Sol. Energy*, 83 (2009) 1485–1498.
- [25] C.J. Popiel, J. Wojtkowiak, Simple formulas for thermophysical properties of liquid water for heat transfer calculations (from 0°C to 150°C), *Heat Transfer Eng.*, 19 (1998) 87–101.
- [26] Y. Raja Sekhar, K.V. Sharma, Study of viscosity and specific heat capacity characteristics of water-based  $Al_2O_3$  nanofluids at low particle concentrations, *J. Exp. Nanosci.*, 10 (2015) 86–102.
- [27] T. Yiamsawasd, A.S. Dalkilic, S. Wongwises, Measurement of specific heat of nanofluids, *Curr. Nanosci.*, 8 (2012) 939–944.
- [28] B.C. Pak, Y.I. Cho, Hydrodynamic and heat transfer study of dispersed fluids with submicron metallic oxide particles, *Exp. Heat Transfer J. Therm. Energy Gener. Transp. Storage Convers.*, 11 (1998) 151–170.
- [29] K. Khanafer, K. Vafai, A critical synthesis of thermophysical characteristics of nanofluids, *Int. J. Heat Mass Transfer*, 54 (2011) 4410–4428.
- [30] H.K. Patel, T. Sundararajan, S.K. Das, An experimental investigation into the thermal conductivity enhancement in oxide and metallic nanofluids, *J. Nanopart. Res.*, 12 (2010) 1015–1031.
- [31] K. Sharma, P. Sharma, W. Azmi, R. Mamat, K. Kadirgama, Correlations to predict friction and forced convection heat transfer coefficients of water based nanofluids for turbulent flow in a tube, *Int. J. Micro-Sci. Nanoscale Therm. Fluid Transport Phenom.*, 3 (2010) 283–308.
- [32] K.S. Wang, J.-H. Lee, S.P. Jang, Buoyancy-driven heat transfer of water-based  $Al_2O_3$  nanofluids in a rectangular cavity, *Int. J. Heat Mass Transfer*, 50 (2007) 4003–4010.
- [33] C.J. Ho, M.W. Chen, Z.W. Li, Numerical simulation of natural convection of nanofluid in a square enclosure: effects due to uncertainties of viscosity and thermal conductivity, *Int. J. Heat Mass Transfer*, 51 (2008) 4506–4516.
- [34] O. Mahian, A. Kianifar, A.Z. Sahin, S. Wongwises, Entropy generation during  $Al_2O_3$  water nanofluid flow in a solar collector: effects of tube roughness, nanoparticle size, and different thermophysical models, *Int. J. Heat Mass Transfer*, 78 (2014) 64–75.
- [35] C.F. Colebrook, Turbulent flow in pipes, with particular reference to the transition region between the smooth and rough pipe laws, *J. Inst. Civ. Eng.*, 11 (1939) 133–156.
- [36] A. Menbari, A.A. Alemrajabi, A. Rezaei, Heat transfer analysis and the effect of CuO/water nanofluid on direct absorption concentrating solar collector, *Appl. Therm. Eng.*, 104 (2016) 176–183.
- [37] G.N. Tiwari, A.K. Tiwari, *Solar Distillation Practice for Water Desalination Systems*, Anamaya Publications, New Delhi, 2007.
- [38] G.N. Tiwari, *Solar Energy: Fundamentals, Design, Modelling and Applications*, CRC Publication/Narosa Publishing House, New Delhi/New York, 2002.
- [39] Dharamveer, Samsher, Comparative analysis of energy matrices and enviro-economics for active and passive solar still, *Mater. Today: Proc.*, 45 (2021) 6046–6052.
- [40] R. Balan, J. Chandrasekaran, S. Shanmugan, B. Janarthanan, S. Kumar, Review on passive solar distillation, *Desal. Water Treat.*, 28 (2012) 217–238.
- [41] H. Prasad, P. Kumar, R.K. Yadav, A. Mallick, N. Kumar, D.B. Singh, Sensitivity analysis of  $N$  identical partially covered (50%) PVT compound parabolic concentrator collectors integrated double slope solar distiller unit, *Desal. Water Treat.*, 153 (2019) 54–64.
- [42] S.K. Sharma, D.B. Singh, A. Mallick, S.K. Gupta, Energy metrics and efficiency analyses of double slope solar distiller unit augmented with  $N$  identical parabolic concentrator integrated evacuated tubular collectors: a comparative study, *Desal. Water Treat.*, 195 (2020) 40–56.
- [43] K. Bharti, S. Manwal, C. Kishore, R.K. Yadav, P. Tiwari, D.B. Singh, Sensitivity analysis of  $N$  alike partly covered PVT flat plate collectors integrated double slope solar distiller unit, *Desal. Water Treat.*, 211 (2021) 45–59.
- [44] D.B. Singh, N. Kumar, Harender, S. Kumar, S.K. Sharma, A. Mallick, Effect of depth of water on various efficiencies and productivity of  $N$  identical partially covered PVT collectors incorporated single slope solar distiller unit, *Desal. Water Treat.*, 138 (2019) 99–112.
- [45] D.B. Singh, A.K. Singh, N. Kumar, V.K. Dwivedi, J.K. Yadav, G. Singh, Performance analysis of Special Design Single Basin Passive Solar Distillation Systems: A Comprehensive Review, A. Prasad, S. Gupta, R. Tyagi, Eds., *Advances in Engineering Design, Lecture Notes in Mechanical Engineering*, Springer, Singapore, 2019, pp. 301–310.
- [46] D.B. Singh, G. Singh, N. Kumar, P.K. Singh, A. Nirala, R. Kumar, Effect of mass flow rate on energy payback time of single slope solar desalination unit coupled with  $N$  identical compound parabolic concentrator collectors, *Mater. Today: Proc.*, 28 (2020) 2551–2556.
- [47] G.K. Sharma, N. Kumar, D.B. Singh, A. Mallick, Exergoeconomic analysis of single slope solar desalination unit coupled with PVT-CPCs by incorporating the effect of dissimilarity of the rate of flowing fluid mass, *Mater. Today: Proc.*, 28 (2020) 2364–2368.
- [48] V.S. Gupta, D.B. Singh, S.K. Sharma, N. Kumar, T.S. Bhatti, G.N. Tiwari, Modeling self-sustainable fully-covered photovoltaic thermal-compound parabolic concentrator s connected to double slope solar distiller, *Desal. Water Treat.*, 190 (2020) 12–27.
- [49] A.K. Singh, D.B. Singh, V.K. Dwivedi, N. Kumar, J.K. Yadav, A Review of Performance Enhancement in Solar Desalination Systems with the Application of Nanofluids, 2018 International Conference on Advances in Computing, Communication Control and Networking (ICACCCN), IEEE, Greater Noida, India, 2018.
- [50] L. Sahota, G.N. Tiwari, Exergoeconomic and enviroeconomic analyses of hybrid double slope solar still loaded with nanofluids, *Energy Convers. Manage.*, 148 (2017) 413–430.
- [51] L. Sahota, Shyam, G.N. Tiwari, Analytical characteristic equation of nanofluid loaded active double slope solar still coupled with helically coiled heat exchanger, *Energy Convers. Manage.*, 135 (2017) 308–326.
- [52] MathWorks Inc., MATLAB-R2016a (9.0.0.341360), 2016.

### Appendix A

$$A_1 = C_1 U_1 + C_2$$

$$C_1 = \alpha_g I_{SE} A_{gE} + U_{cgaE} A_{gE} T_a$$

$$C_2 = \alpha_g I_{SW} A_{gE} A_{gW} h_{EW} + U_{cgaW} A_{gE} T_a A_{gW} h_{EW}$$

$$U_1 = h_{1wE} \frac{A_b}{2} + h_{EW} A_{gE} + U_{cgaE} A_{gE}$$

$$A_2 = (h_{1wE} U_2 + h_{1wW} h_{EW} A_{gE}) \frac{A_b}{2}$$

$$U_2 = U_{cgaW} A_{gW} + h_{1wW} \frac{A_b}{2} + h_{EW} A_{gW}$$

$$B_1 = C'_1 U_1 + C'_2$$

$$B_2 = (h_{1wW} U_1 + h_{1wE} h_{EW} A_{gE}) \frac{A_b}{2}$$

$$C'_1 = \alpha_g I_{SW} A_{gE} + U_{cgaW} A_{gE} T_a A_{gW}$$

$$C'_2 = \alpha_g I_{SE} A_{gE} A_{gW} h_{EW} + U_{cgaE} A_{gE} T_a A_{gW}$$

$$D_3 = m_f C_f [T_{HE} - T_{wi}]$$

$$D_1 = \left[ \frac{(AF_R(\alpha\tau))1(1-K_p^N)}{(1-K_p)} \left( 1 - \frac{1}{(1-e^z K_m^N)} \right) \right]$$

$$D_2 = \left[ \frac{(AF_R(UL))1(1-K_p^N)}{(1-K_p)} \left( 1 - \frac{1}{(1-e^z K_m^N)} \right) \right]$$

$$E_1 = U_{gaW} \left[ h_{EW} + h_{1bwE} \left( \frac{A_b}{2A_{gE}} \right) \right]$$

$$E'_1 = U_{gaW} \left[ h_{EW} + h_{1bwE} \left( \frac{A_b}{2A_{gE}} \right) \right]$$

$$E_2 = U_{gaW} (h_{EW} + U_{gaE}) A_{gE} A_{gW}$$

$$E'_2 = U_{gaE} (h_{EW} + U_{gaW}) A_{gE} A_{gW}$$

$$H_1 = (U_{gaE} + U_{gaW}) h_{1bwW} h_{1bwE} \left( \frac{A_b}{2} \right)$$

$$H_2 = A_{gE} A_{gW} h_{EW} (U_{gaE} h_{1bwE} + U_{gaW} h_{1bwW})$$

$$H_3 = A_{gE} A_{gW} U_{gaE} U_{gaW} (h_{1bwE} + h_{1bwW})$$

$$H_4 = A_{gE} A_{gW} h_{EW} (U_{gaE} h_{1bwW} + U_{gaW} h_{1bwE})$$

$$H'_{11} = H_1 + H_2 + H_3 + H_4$$

$$H'_{33} = U_b A_b - D_1$$

$$H'_{44} = U_b A_b + D_3$$

$$K_{1E} = \left[ h_{1bwW} \left( \frac{A_b}{2A_{gW}} \right) + h_{EW} \left( 1 + \frac{1}{h_{1bwE}} \right) + U_{gaW} \right] A_{gW} \alpha_g A_{gE} h_{1bwE}$$

$$K_{1W} = \left[ h_{1bwE} \left( \frac{A_b}{2A_{gE}} \right) + h_{EW} \left( 1 + \frac{1}{h_{1bwW}} \right) + U_{gaE} \right] A_{gW} \alpha_g A_{gE} h_{1bwW}$$

$$K'_{1E} = \left[ h_{1bwW} \left( \frac{A_b}{2} \right) + h_{EW} \left( 1 + \frac{h_{1wE}}{h_{1wW}} \right) A_{gW} + U_{gaW} A_{gW} \right] \alpha_g A_{gE} h_{1wE}$$

$$K'_{1W} = \left[ h_{1bwE} \left( \frac{A_b}{2} \right) + h_{EW} \left( 1 + \frac{h_{1wE}}{h_{1wW}} \right) A_{gE} + U_{gaE} A_{gE} \right] \alpha_g A_{gW} h_{1wW}$$

$$P = U_1 U_2 - h_{EW}^2 A_{gE} A_{gW}$$

Expressions for  $K_p$ ,  $(AF_R(\alpha\tau))_1$  and  $(AF_R U_L)_1$  used in Eq. (1) are as follows.

$$K_p = 1 - \frac{(AF_R(UL))1}{m_f C_f}$$

$$K_m = 1 - \frac{(A_{rm} F_{Rm}(UL)m)}{m_f C_f}$$

$$U_{tca} = \left[ \frac{1}{h_o} + \frac{L_g}{K_g} \right]^{-1}; \quad U_{tcp} = \left[ \frac{1}{h_i} + \frac{L_g}{K_g} \right]^{-1};$$

$$h_o = 5.7 + 3.8V, \quad \text{Wm}^{-2}\text{K}^{-1}; \quad V = 1 \text{ ms}^{-1}; \quad h_i = 5.7, \quad \text{Wm}^{-2}\text{K}^{-1};$$

$$U_{tpa} = \left[ \frac{1}{U_{tca}} + \frac{1}{U_{tcp}} \right]^{-1} + \left[ \frac{1}{h'_i} + \frac{1}{h_{pf}} + \frac{L_i}{K_i} \right]^{-1};$$

$$h'_i = 2.8 + 3V', \quad \text{Wm}^{-2}\text{K}^{-1};$$

$$U_{L1} = \frac{U_{tcp} U_{tca}}{U_{tcp} + U_{tca}}; \quad U_{L2} = U_{L1} + U_{tpa}; \quad U_{Lm} = \frac{h_{pf} U_{L2}}{F' h_{pf} + U_{L2}};$$

$$U_{Lc} = \frac{h_{pf} U_{tpa}}{F' h_{pf} + U_{tpa}};$$

$$PF_1 = \frac{U_{tcp}}{U_{tcp} + U_{tca}}; \quad PF_2 = \frac{h_{pf}}{F' h_{pf} + U_{L2}}; \quad PF_c = \frac{h_{pf}}{F' h_{pf} + U_{tpa}};$$

$$(\alpha\tau)_{1\text{eff}} = \rho(\alpha_c - \eta_c)\tau_s\beta_c \frac{A_{\text{am}}}{A_{\text{rm}}}; \quad (\alpha\tau)_{2\text{eff}} = \rho\alpha_p\tau_s^2(1-\beta_c) \frac{A_{\text{am}}}{A_{\text{rm}}};$$

$$(\alpha\tau)_{\text{meff}} = [(\alpha\tau)_{1\text{eff}} + \text{PF}_1(\alpha\tau)_{2\text{eff}}]; \quad (\alpha\tau)_{\text{ceff}} = \text{PF}_c \cdot \rho\alpha_p\tau_s \frac{A_{\text{ac}}}{A_{\text{rc}}};$$

$$(AF_R(\alpha\tau))_1 = \left[ A_c F_{\text{Rc}}(\alpha\tau)_{\text{ceff}} + \text{PF}_2(\alpha\tau)_{\text{meff}} A_m F_{\text{Rm}} \left( 1 - \frac{A_c F_{\text{Rc}} U_{\text{Lc}}}{\dot{m}_f C_f} \right) \right];$$

$$(AF_R U_L)_1 = \left[ A_c F_{\text{Rc}} U_{\text{Lc}} + A_m F_{\text{Rm}} U_{\text{Lm}} + A_m F_{\text{Rm}} U_{\text{Lm}} \left( 1 - \frac{A_c F_{\text{Rc}} U_{\text{Lc}}}{\dot{m}_f C_f} \right) \right]$$

$$A_{\text{rm}} = b_r L_{\text{rm}}; \quad A_{\text{am}} = b_o L_{\text{am}};$$

$$A_c F_{\text{Rc}} = \frac{\dot{m}_f C_f}{U_{\text{Lc}}} \left[ 1 - \exp\left( \frac{-F' U_{\text{Lc}} A_c}{\dot{m}_f C_f} \right) \right];$$

$$A_m F_{\text{Rm}} = \frac{\dot{m}_f C_f}{U_{\text{Lm}}} \left[ 1 - \exp\left( \frac{-F' U_{\text{Lm}} A_m}{\dot{m}_f C_f} \right) \right];$$

$$z = \frac{2\pi r_{11} U_L}{\dot{m}_f C_f}$$